Chemical synthesis using a non-thermal pin-to-plate microsecond pulsed DBD reactor

Avishek Banerjee

Department of Chemical Engineering
McGill University
Montréal, Québec, Canada

August 12, 2022

A thesis presented for the degree of Master of Science in Chemical Engineering

Abstract

In this thesis, plasma-chemical synthesis of fuels and valuable chemicals was investigated. Reforming processes is the backbone for transforming heavy oils into valuable fuels that sustains our energy consumption. Conventional processes, like fluid catalytic cracking or steam reforming, generate huge amounts of CO_2 and is a major contributor to greenhouse gas (GHG) emissions. Several efforts to tackle climate change and recent focus on sustainable energy solutions has enhanced the need to produce CO_2-free fuels or look into alternate pathway of producing chemical energy. Thus non-thermal plasma (NTP), known to have the ability to produce CO_2-free fuels, was studied. The ability for NTP to produce energetic electrons while keeping the gas at room temperature is unique and is crucial for enabling thermodynamically unfavorable reactions to proceed at room temperature.

A pin-to-plate non-thermal plasma reactor was designed and constructed to understand the mechanisms of plasma-liquid interactions in the context of organic synthesis. A microsecond pulsed plasma was chosen due to its known energy efficiency along with argon as the carrier gas for its operation. The vapor pressure and the dielectric permittivity of the liquids used were observed to have an influence on the breakdown voltage. To this regard, the temperature in our studies was maintained to have minimum temperature rise of the liquid and to gain more transparent knowledge of the plasma-chemistry. Further, alcohols were added to hydrocarbons to understand if reaction paths are altered by additives.

The gas and liquid products obtained from the plasma synthesis were characterized using GC-TCD and the liquid products were characterized using GC-MS. Thorough chemical assessments of the products obtained were conducted to understand the conversion efficiency of our reactor. The results obtained showed that it is possible for the proposed reactor to simultaneously synthesize H_2 and/or syngas, crack heavy oils as well as produce more complex valuable liquid chemicals.

In our NTP reactor, the treatment temperatures used were kept constant at 20 °C, 0 °C, and -20 °C to keep the vapor pressure constant throughout the treatment. The highest conversion of 771.4 mmol/kWh was achieved for hexane-ethanol mixture at 0 °C. It was also concluded that the production of H_2 and other lower fuels can be increased by the addition of alcohols. At 0 °C the production efficiency of gas products was found to be higher compared to other temperatures. For liquid products, lower temperatures showed higher production efficiency with -20 °C having the highest efficiency. Product formation was observed to mainly undergo dissociation and dehydrogenation, whose reaction pathway was also discussed.

Abrégé

Dans cette thèse, la synthèse plasma-chimique de carburants et de produits chimiques à grande valeur ajoutée a été étudiée. Les processus de reformage sont l'épine dorsale de la transformation des huiles lourdes en carburants à grande valeur ajoutée qui soutiennent notre consommation d'énergie. Les procédés conventionnels, tels que le craquage catalytique fluide ou le reformage à la vapeur, génèrent d'énormes quantités de CO_2 et sont un contributeur majeur aux émissions de gaz à effet de serre (GES). Plusieurs efforts pour lutter contre les changements climatiques et l'accent mis récemment sur les solutions énergétiques durables ont renforcé la nécessité de produire des carburants sans émissions de CO_2 ou de rechercher des sources d'énergie alternatives. Ainsi, les plasmas non-thermique (PNT), dont on sait qu'ils ont la capacité de produire des carburants sans CO_2, a été étudié. La capacité du PNT à produire des électrons énergétiques tout en maintenant le gaz à température ambiante est unique et est cruciale pour permettre aux réactions thermodynamiquement défavorables de se dérouler à température ambiante.

Un réacteur à plasma non thermique point-plan a été conçu et construit pour comprendre les mécanismes des interactions plasma-liquide dans le contexte de la synthèse organique. Un plasma pulsé microseconde a été choisi en raison de son efficacité énergétique connue avec l'argon comme gaz vecteur pour son fonctionnement. On a observé que la pression de vapeur et la permittivité diélectrique des liquides utilisés avaient une influence sur la tension de claquage. À cet égard, la température dans nos études a été contrôlée pour avoir une élévation de température minimale du liquide et pour acquérir une meilleure connaissance de la chimie du plasma. De plus, des alcools ont été ajoutés aux hydrocarbures pour comprendre si les voies de réaction sont modifiées par des additifs.

Les produits gazeux obtenus à partir de la synthèse du plasma ont été caractérisés par GC-TCD et les produits liquides ont été caractérisés par GC-MS. Des évaluations chimiques approfondies des produits obtenus ont été menées pour comprendre l'efficacité de conversion de notre réacteur. Les résultats obtenus ont montré qu'il est possible pour le réacteur proposé de synthétiser simultanément du H_2 et/ou du gaz de synthèse, de craquer des huiles lourdes et de produire des produits chimiques liquides à grande valeur ajoutée plus complexes.

Dans notre réacteur NTP, les températures de traitement utilisées ont été maintenues constantes à 20 °C, 0 °C, -20 °C pour maintenir la pression de vapeur constante tout au long du traitement. La conversion la plus élevée de 771,4 mmol/kWh a été obtenue pour le mélange hexane-éthanol à 0 °C. Il a également été conclu que la production de H_2 et d'autres carburants inférieurs peut être augmentée par l'ajout d'alcools. À 0 °C, l'efficacité de la production de produits gazeux s'est avérée supérieure à celle des autres températures. Pour les produits liquides, des températures plus basses ont montré une efficacité de production plus élevée, -20 °C ayant l'efficacité la plus élevée. Il a été observé que la formation des produits procède principalement par une dissociation et une déshydrogénation, dont la voie de réaction est également discutée.

Acknowledgements

First and foremost I would like to thank my supervisor, *Prof. Pierre-Luc Girard-Lauriault*, for opening up the doors of McGill for my masters. It was due to his support and advice that I believed more in my project and was able to discover what I would like to work on in the future. Thank you so much for being such a great and friendly supervisor, and for assisting me throughout this journey, and for making my experience fruitful. Without you this thesis wouldn't have been possible.

I would also thank all the McGill staff, the Wong Workshop, the Chemical Engineering Store, the Electrical Shop, and the Analytical Lab for providing every help possible in every step. Special mention to *Andrew Golsztajn*, for being there with me almost the entire day for weeks when I was not sure how things would work. Your training and advice have made me a more knowledgeable person in the analytical lab, and yes, now I know a lot about all the different GCs.

Next, I would thank my present and past lab mates, *Dr. Balaji Ramachandran, Olivia, Jessica, Saad* and especially, *Bishakh Rout* with whom I shared my office space for the entire

duration of my masters. Thank you all for keeping a lively and enriching work environment. Also, I would like to thank *Alexandre Leblond*, my summer student, for working with me simultaneously and helping me design and build a significant portion of the reactor.

Thank you to all the friends I made here in Montreal. *Siril*, *Sripadh*, *Rahul*, and *Fathima*, you guys are great friends and it was always fun to hang out together. Thank you *Shreya* for always reminding me of my hometown, and obviously for all the things you got me from back home. Special mention to *Anirban Kundu*, you are an inspiration and I always learn from you. Our coffee breaks and *"adda"* is what kept me going. They helped me discover myself, and different opportunities, and more importantly, were a stress reliever in between work. All my friends in India and around the world, thank you for always being my go-to people. Last but not the least, thank you *Antara Paul*, for being there with me through thick and thin. You gave me the strength to fight the ups and downs of life. You gave me joy and happiness and I am fortunate to have met and known you.

I would like to thank all the teachers and professors from my high school and undergraduate. You made me what I am today, so thank you very much!

Finally, I would like to thank my parents without whom any of this would not have been possible. You inspire me to work hard every day and I hope to make you proud through this thesis. This thesis is dedicated to both of you!

Contents

3 Plasma synthesis of chemicals from liquid organic compounds 29

List of Figures

List of Tables

List of Acronyms

η_g	production efficiency of gas (mmol/kWh).
η_l	production efficiency of liquid (g/kWh).
DBD	dielectric barrier discharge.
FCC	fluid catalytic cracking.
GAD	gliding arc reactor.
GC-MS	gas chromatography - mass spectrometry.
GC-TCD	gas chromatography - thermal conductivity detector.
HC	hydrocarbon.
HV	high voltage.
LIBS	laser-induced breakdown spectroscopy.
MALDI	matrix-assisted laser desorption ionization.
NTP	non-thermal plasma.
PAW	plasma activated water.
RONS	reactive oxygen and nitrogen species.

Chapter 1

Introduction

1.1 Project Motivation

The clean production of fuel has received increased interest in the past few years as the world is looking to move towards cleaner and greener forms of energy. Current practices comprise steam reforming or FCC processes that are both energy-intensive and emit large amounts of CO_2 into the environment [1]. CO_2 is also the major greenhouse gas responsible for climate change with an emission of 37.1 Gt CO_2/year from fossil fuels alone [2]. Thus, the need for a carbon-neutral technology has led to new investigations.

New technologies that are emerging are radiation processing [3, 4], biochemical conversion [5], and photochemical conversion [6], however, they are far away from industrial implementation. Radiation processing either requires higher temperatures of 350

°C or a very high dose rate of 10kJ/kg-s or more, and biochemical/photochemical processes typically have low power density. Whereas, NTP methods can be portable, scalable, or modular units, and are capable of supplying a higher power density. They are more economical with a low energy cost (1-3 eV/molecule) due to their ambient operating conditions and are less sensitive to impurities than catalytic processes [7]. Recent investigations on the role of gas temperature and energetic electrons in plasma chemistry have thus opened new paths of exploration involving reforming processes [8].

NTP has been previously used for fuel gas treatment and has been very attractive for its non-equilibrium nature. Its ability to induce chemical reactions at low temperatures makes it an interesting prospect for organic synthesis processes. The electrons in NTP are usually at a high temperature of 1-10 eV whereas, the gas stays at room temperature. This unique advantage consumes less power and energy and enables thermodynamically unfavorable reactions to proceed at room temperature [9]. It is further portable and can work in-situ. Also, recently it has been regarded as a flexible technology that can store and use intermittent renewable electricity to convert electrical energy into chemical energy [10].

In this context, this thesis presents the use of non-thermal plasma as a sustainable technology for fuel reforming. A gas discharge over liquid, DBD reactor was constructed which is more economical than other kinds of discharges (discussed in Chapter 2). The products exiting from the gas phase and the products formed in the liquid phase were studied to gain information on the plasma-liquid interface chemistry. The thesis highlights the use of NTP as a technology to simultaneously synthesize H_2 or syngas, crack heavy HCs, and produce more valuable complex chemicals.

1.2 Objectives

The main objective of the thesis was to develop a plasma reactor to understand the plasma-liquid interactions at the gas-liquid interface and for the synthesis of organic compounds. To achieve this main objective, the following specific steps were addressed:

1. Design and construction of a microsecond pulsed non-thermal pin-to-plate plasma reactor.
2. Establish methods for characterization of the gas and liquid products, both of which are complex mixtures containing a variety of organic compounds and some inorganic gases like H_2 and CO.
3. To use a simple model hydrocarbon and study the different gas and liquid products formed from it and optimize the operating conditions of the reactor.
4. Add alcohols to the hydrocarbon and study the change in the reaction chemistry of the mixture and consequently, the products formed.

1.3 Thesis Outline

This manuscript-based thesis is comprised of 4 chapters. Chapter 1 describes the project motivation and a brief insight into the work carried out. Chapter 2 summarizes the literature concerning the background of this project. It includes an overview of the fundamentals of plasma–liquid interactions, followed by an overview of the reforming of fuels, with a particular focus on plasma reforming. The body of this work, Chapter 3, is composed of a manuscript accepted for publication in a peer-reviewed scientific journal *(ACS Sustainable Chemistry & Engineering)*. It describes an NTP reactor for plasma-chemical interactions of n-hexane and its mixture with methanol and ethanol, and focuses on the gas and liquid products formed, along with the conversion efficiency of the proposed reactor. Finally, Chapter 4, comprises a short discussion of the overall thesis, with a closing section that summarizes the conclusions and contributions to knowledge that can be drawn from this work, along with recommendations for future work.

Chapter 2

Background

2.1 Plasma-liquid interactions

2.1.1 Introduction to plasma-liquid interactions

In the past, research on non-thermal plasma has been associated with gas-phase discharges, however, with recent advances in plasma science, and especially with the growing interest in non-thermal plasma for several applications, plasmas generated in the liquid-phase or interfacing with the liquid has attracted growing interest. The complex chemistry in this multiphase phenomenon remains vastly unexplored and provides a rich field of investigation [11].

Plasma-liquid systems are classified based on their reactor geometries and the kind of discharge that occurs in the system. Similar to gas-phase plasmas, they have a few classification schemes which can be described as follows (Figure 2.1) [12].

- Direct discharge inside the liquid medium
- Discharge over the liquid with the plasma producing reactivity in the bulk
  - Without direct contact/electrical coupling with the liquid
  - With direct contact/electrical coupling with the liquid (liquid electrode)
  - At the plasma liquid interphase (surface discharges)
- Multiphase plasmas including
  - Gas phase plasmas with dispersed liquid phase (aerosols)
  - Gas phase plasmas dispersed in the gas phase (bubbles) in liquid

In-liquid discharges (Figure 2.1A) require a high breakdown electric field due to the higher density of liquids than gases. Discharges formed in liquid are believed to follow either an electron-induced mechanism [13], where a high electric field leads to liquid ionization, or a gas bubble mechanism [14], where a low density region is formed in the liquid just before plasma initiation. These mechanisms have been able to achieve plasma initiation for up to microsecond scale and are energy-intensive. For instance, under ambient conditions, the breakdown electric field for distilled water is 0.4 MV cm^{-1} whereas for argon it is 0.3 kV cm^{-1} [15,16]. Similarly, with multiphase bubble/aerosol discharges (Figure 2.1 E-F), there remain a few drawbacks, where the electron density significantly varies with the excitation

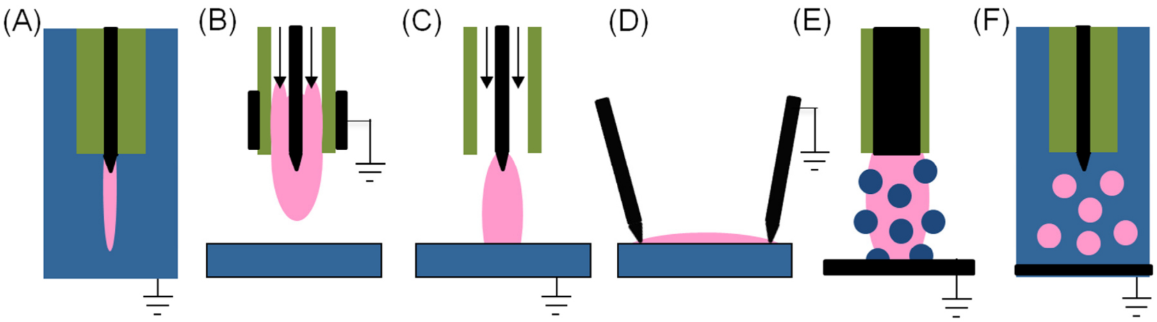

Figure 2.1: Classification of different types of plasma-liquid discharge (A) direct discharge inside the liquid medium, (B)–(D) gas phase discharges and (E) and (F) multiphase discharges. In more detail: (B) plasma jet without direct contact with liquid, (C) gas phase plasma with liquid electrode, (D) surface discharge, (E) gas phase plasma with dispersed liquid phase (aerosols) and (F) discharges in bubbles. Blue = liquid, pink = plasma, green = dielectric, black = metal electrodes, has been adapted from [12].

voltage, discharge power, conductivity of the liquid, and size of the bubble [9]. Thus there has been an increased interest in gas discharge over liquids in recent years [17, 18].

2.1.2 Gas discharge over liquids

Gas discharges are particularly interesting due to their low energy requirement, owing to their low breakdown voltages. In such discharges, the high voltage (HV) electrode is usually in the gas phase, and the other electrode is either the liquid itself or a conducting metal submerged inside the liquid, as shown in Figure 2.2. The plasma generated is surrounded by gas, produced from the liquid interface and the vapor of the liquid [19].

Figure 2.1 B. shows a plasma jet in which the gas enters through a concentric electrode, where the inner pin is the high voltage, and the outer dielectric barrier electrode is grounded.

Figure 2.2: DC driven air glow discharge in a pin-water geometry with self-organization at the surface of the water anode electrode, has been adapted from [20].

This configuration creates a high electric field for the gas to ionize and transfer a stream to reactive species to the liquid interface [21]. Figure 2.1 C. shows a pin to liquid electrode, where the liquid act as the ground electrode and the discharge hits directly on the surface of the liquid. It was further determined, that the polarity of the liquid (cathode/anode) can influence the plasma discharge characteristics [22]. Figure 2.1 D. shows two electrodes, both at the surface of the liquid, where the electrons can propagate along the surface. Another type of discharge could be a dielectric barrier discharge (DBD), which is also our setup, where the HV electrode is in the air, the ground electrode is inside the liquid, and the liquid itself acts as the dielectric barrier, as shown in Figure 2.3 [23]. These discharges are promising as they do not allow sparks or arc formation and are more uniform than other kind of discharges [24].

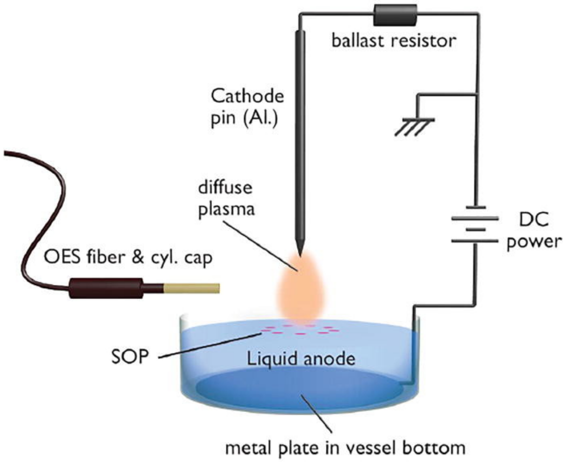

Figure 2.3: A typical pin-to-plate dielectric barrier discharge plasma, has been adapted from [23].

2.1.3 Relevance of using microsecond pulsed pin-to-plate discharge

Although discharges in gas-liquid environments are known to be more energy-efficient, the type of discharge also determines the energy consumption of the system. The electric field generated between the two electrodes should be high enough to initiate gas ionization/reactive species while reducing energy wastage at the same time, for example, heating up of the gas and liquid. A pulsed power supply can be helpful in this regard as it results in a system that produces more excitation, ionization, and sputtering, at similar or lower average power, compared to traditional continuous AC or DC operation [25].

Research on pulsed power supply mainly comprises millisecond, microsecond, and nanosecond plasma. Millisecond plasma was found to be weak, and with higher frequency of pulses, the discharge region would get hot, which reduces energy efficiency [26]. They are also low in space charge density and cannot maintain a high electric field throughout the time of plasma discharge. Nanosecond pulses, which generate large amounts of discharge energy, changes the electrical characteristics of the system over time due to changing pressure and air density in the system, and they also tend to cause electromagnetic interference with other equipment connected to the system [27, 28]. Thus, the disadvantages of millisecond and nanosecond plasma have opened up more investigations on microsecond discharges. Furthermore, microsecond pulsed plasma discharges have a lower energy consumption than millisecond discharge and have less electromagnetic interference than nanosecond discharge, making it more suitable for engineering applications [29].

Recently a few successful studies in gas-liquid environments have been carried out with microsecond pulsed plasma which include studies on plasma-activated water [18, 30, 31], hydrocarbon reforming [32, 33], decontamination of water [34, 35] and so on. Commercially available microsecond pulsed plasma supply, like the G2000 used in our experiments, further makes it accessible for NTP applications. Thus the choice to use microsecond pulsed plasma discharge was made for fuel reforming applications in our work.

2.1.4 Chemistry at the plasma-liquid interface

The chemistry of plasmas in contact with liquids is complex and requires a deeper understanding. For instance, in an atmospheric plasma jet, one may need to consider (a) an inert gas initiating a plasma, which interacts with the gas phase of increasing humidity as water or other liquid surface is approached, (b) the impact of charged and neutral particles and photons and penetration or migration of these species through the water surface, (c) the neutral and ion chemistry of short and long-lived species immediately below the surface and (d) the resultant bulk liquid chemistry. In each of these environments, the user community should estimate typical time scales, major expected species and define the dominant collision regimes (e.g. ion-neutral, neutral-neutral, radical-radical or radical-neutral, solvation or clustering) to help guide the production of data [12].

The interaction of the ionized gas with the surface of the liquid involves several kinetic and transport processes. The main processes are gas kinetic collisions, adsorption onto the particle surface (aerosol), absorption into the bulk of the particle, desorption from the surface, bulk diffusion in the condensed phase, and chemical reactions at the surface of the particle or in the bulk of the particle, as shown in Figure 2.4 [36]. The main drivers of these processes and reactions are the ions and electrons, generated by a high electric field.

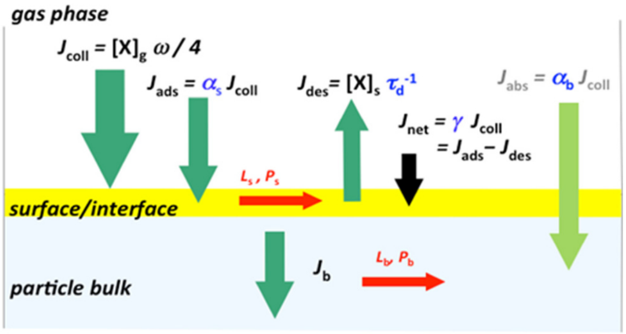

Figure 2.4: Schematic of key processes and fluxes in the gas uptake by atmospheric particles: gas kinetic flux of surface collisions (Jcoll), adsorption onto the particle surface (Jads), absorption into the particle bulk (Jabs), desorption from the surface (Jdes), and net uptake by the condensed phase (Jnet). The red arrows indicate production and loss of chemical species by reactions at the particle surface (Ps, Ls) or in the particle bulk (Pb, Lb). [X]g and [X]s are the gas and surface concentrations, has been adapted from [36].

Ions

Ions can be both cations and anions. It is assumed, that cations have high potential energy to overcome any activation energy barriers like surface tension at the interface and are easily solvated when striking the liquid. Anions, on the other hand are much less understood. Although they are energetically analogous to neutral species, they are more polarizable than neutrals or cations and can penetrate into the liquid. However, the reverse mechanism, of whether the cations leave the liquid is not well known. The ion energy required to transfer the oxidative power of the plasma to the liquid is equal to the ion mean-free path. Also, UV photons can provide some energy to the system, in which case less ion energy is required [12].

Electrons

Electron-induced reactions at the liquid interface can be generally classified into two types: (a) highly energetic electrons which could (vibrationally) excite, dissociate (including dissociative attachment) or ionize water molecules, and (b) low energetic electrons which adsorb and absorb, and eventually become solvated electrons ($e^-_{(\mathrm{gas})} \rightarrow e^-_{(\mathrm{aq})}$) [12]. The lifetime of the solvated electrons is not clearly understood, and there are many reactions of solvated electrons as reported in radiation chemistry literature [37]. The effectiveness of these reactions depends upon the pH, temperature, presence of solvated electron scavengers, dissolved gases, and concentration of the solvated electrons [38]. The energy with which the electrons strike the interface also determines whether a product at the interface will go into the gas-phase or liquid-phase [39].

2.1.5 Applications of plasma-liquid system

Several applications have emerged in the last decade based on plasma-liquid interactions, like nanomaterial processing, analytical chemistry, organic wastewater treatment, plasma sterilization and disinfection, biomedical applications, plasma agriculture, and plasma for reforming reactions.

Nanomaterial Processing

Plasma-liquid interactions have been extensively researched in the recent past for nanoparticle synthesis. Wet chemical methods which work on the principle of chemical reduction with a reducing agent, although efficient, suffer from long processing times. Whereas in plasma-assisted synthesis, the energetic electrons act as reducing agents and are produced on-site, which is a key advantage of this process [40, 41]. Significant attention has been paid to producing gold and silver nanoparticles with different kind of plasma discharges including, DC discharges [42], micro-plasma discharges [43] and pulsed discharges [44–47]. Studies have also been extended to copper nanoparticles and other metals as well [48–50]. Although it is a well-established field, for both nanoparticles and surface functionalization, further investigations are still being carried out to understand the complex plasma-induced physical and chemical phenomena.

Analytical Chemistry

Plasma has been used in analytical chemistry to analyze various samples of solid, liquid, and gas. Inductively coupled plasma is the most commonly used, which works under electromagnetic induction in an Ar atmosphere. The liquid sample can be introduced by thermal vaporization, electro-thermal vaporization, laser ablation, or liquid spraying using a nebulizer [51]. It is used in other analytical techniques as well, like mass spectrometry or radiation spectroscopy. Different ionization processes are used to transfer the sample to a plasma state, matrix-assisted laser desorption ionization (MALDI), electrospray ionization, and laser-induced breakdown spectroscopy (LIBS) [52]. Among these, LIBS stands out due to its ability to take measurements from samples remotely, which aligns with the recent trends of miniaturizing and modularizing equipment [53]. Furthermore, direct plasma discharge on liquids is also possible for analytical measurements, for instance, in electrolyte-cathode discharge (ELCAD) spectroscopy, metal ions from an electrolytic solution, which serves as the cathode, are transferred to a contacting DC glow discharge by cathode sputtering [54]. Investigations on underlying mechanisms for atomization and excitation are still carried out to get a clearer understanding of such techniques.

Organic Wastewater Treatment

Tertiary treatments in wastewater mainly consist of advanced oxidation processes, like ozonation or UV-based lamps, which are accompanied by H_2O_2. H_2O_2 is unfortunately a difficult compound for storage and handling. Plasma treatment of water provides a suitable alternative as it can produce reactive species like ozone, H_2O_2, and UV photons on-site. The oxidation processes can be initiated by O_3, H_2O_2, $OH\bullet$ radicals, and atomic oxygen $O(^3P)$ that can either be produced at the gas phase and transferred to the bulk of the liquid or can be directly produced inside the liquid [52]. In recent years a few studies have focused on the removal of various organic pollutants like pesticides, pharmaceuticals, and personal-care products [55–57].

Sterilization and Disinfection

Although many studies exist for plasma sterilization of microorganisms under dry conditions, sterilization in wet conditions is relatively new [58]. In wet sterilization process, the microorganisms are believed to have an additional barrier, which is the liquid itself. However, it has been found, that sterilization is possible under wet conditions with the use of plasma. The main reactive species responsible are O_3, H_2O_2, $OH\bullet$ radicals, and atomic oxygen $O(^3P)$ formed in water, which directly attacks the cells of the microorganisms and inactivates them [59]. It is also believed that acidification of the water, mainly by nitrate compounds from plasma treatment, also plays a role in sterilization. Recent studies investigate the inactivation of different bacteria like *S. aureus, E. faecalis, E. coli, P. aeruginosa, MRSA, M. terrae, M. abscessus, B. cereus, C. albicans, T. mentagrophytes, and A. niger* under different types of plasma discharge [60–62].

Biomedical Applications

Due to the ambient operating conditions of non-thermal plasmas, they are suitable for treating vulnerable living cells and tissues. Plasma-generated RONS species have high antimicrobial, anti-cancer, and chronic wound healing effects and can induce certain chemical and biological reactions inside cells and tissues [63]. Treatments are either direct or indirect depending on the plasma contact with cells. Besides RONS, UV radiation was also found to be effective in biomedicines. Different biomedical applications include prevention of post-surgical infections, non-inflammatory tissue regeneration, oncology, chronic wound healing, treatment of skin diseases, cancer therapy, dental caries, etc [64].

Plasma Agriculture

Plasma has been previously used to treat cells, and for soil remediation [65, 66]. However, its most noticeable application in agriculture is PAW for use with plants [67, 68]. PAW can be considered a fertilizer, as the NO_3^- groups which provide a rich source of nitrogen compounds and the acidic water both helps in plant growth. Other non-thermal technologies like ozonation, chemical treatment, high-pressure processing, or UV irradiation have also been explored, but they possess disadvantages, like higher processing time, high equipment cost, low efficiencies, and undesirable residues, which brings plasma treatment to the focus [69]. Studies conducted with different kinds of non-thermal plasma showed different efficacy due to the different chemical compositions of PAW. Plant growth was further verified by researchers on different plants, like radish, tomato, sweet potato, etc., where all showed increased growth compared to tap water [67, 70].

Plasma-Fuel Reforming

Conventional methods of reforming and their drawbacks of high CO_2 emissions have forced the research community to investigate innovative ways of reforming. NTP technology has come to the forefront owing to its ambient operating conditions, no catalyst requirement, portability, and the ability for in-situ operation. Several projects involving research on different kinds of plasma discharges for fuel reforming is ongoing. Section 2.2 further elaborates on the use of NTP for such processes.

2.2 Reforming of Fuels

Fuel reforming reactions are mostly catalytically driven to form hydrogen-rich mixtures. Conventional methods like steam reforming, autothermal reforming, and partial oxidation are energy-intensive with a requirement for catalyst deactivation along with high CO_2 emissions. Such processes are largely commercialized in today's world with benefits in terms of efficiency, but their drawbacks pose a major threat to the environment as listed in Table 2.1 [71].

Table 2.1: Benefits and drawbacks of selected fossil fuel reforming methods, has been adapted from [71].

Technology	**Benefits**	**Drawbacks**
Steam Reforming	Highly industrial process No oxygen input needed lowest operating temperatures Highest H_2/CO ratio	Highest greenhouse gas (GHG) emissions
Autothermal Reforming	Operating temperature lower than partial oxidation	Limited commercial experience

	Less methane slip	Air/oxygen requirement
Partial Oxidation	Fewer desulfurization needs	Low H_2/CO ratio
	No catalyst requirement	High operating temperatures
	Less methane slip	Complex handling process

These drawbacks have further enhanced the need for a clean process in the fuel reforming industries. Various emerging processes, like biochemical/photochemical conversion and radiation processing are not used at industrial scales due to their low efficiency and high energy requirements. Thus, non-thermal plasma can be a suitable alternative to replace conventional methods, and its investigation can provide us with critical insight, discussed in the upcoming chapters.

2.2.1 Plasma chemistry in fuel reforming processes

Chemical reactions driven by plasma can be associated to mainly three regimes: (I) strongly exothermic reactions, (II) endothermic reactions, and (III) weakly exothermic reactions. Regimes (I) and (III), although mostly associated with “warm plasmas”, can affect the ionization path and oxidation capabilities of the non-thermal plasma processes as well [72].

Strongly Exothermic Reactions

These kind of reactions are mostly associated with plasma-assisted combustion, which is also an emerging field. In this regime, plasma chemistry and thermochemistry are discernible. Charged particles from the plasma have a very short lifetime, usually from nanosecond to millisecond range. However, radicals and electron-induced ions, like O, have a longer lifetime and can initiate a reaction. O can be generated by dissociation of O_2 by electrons (Equation 2.1) and excited Ar. (Equations. 2.2, 2.3) [73],and vibrationally excited O_2 can be generated by vibrationally excited N_2 (Equations. 2.4, 2.5) [74].

$$\mathrm{e} + \mathrm{O_2} \longrightarrow \mathrm{O}\,(^3\mathrm{P}) + \mathrm{O}\,(^1\mathrm{D}) \tag{2.1}$$

$$\mathrm{Ar} + \mathrm{e} \longrightarrow \mathrm{Ar}^* + \mathrm{e} \tag{2.2}$$

$$\mathrm{Ar}^* + \mathrm{O_2} \longrightarrow \mathrm{Ar} + 2\,\mathrm{O} \tag{2.3}$$

$$\mathrm{N_2}(v = 0) + \mathrm{e} \longrightarrow \mathrm{N_2}(v > 0) + \mathrm{e} \tag{2.4}$$

$$\mathrm{N_2}(v) + \mathrm{O_2}(v' = 0) \longrightarrow \mathrm{N_2}(v - 1) + \mathrm{O_2}(v' = 1) \tag{2.5}$$

Once the reactions are initiated, small changes in electrical power, although changes the efficiency of production, do not change the end products. Thus it is difficult to effectively determine the cost-efficiency of these processes.

Endothermic Reactions

Thermal energy is not available with non-thermal plasmas, so the main energy transfer is driven by electrons. The most common example of such reactions is dry reforming of HCs by CO_2+CH_4. The first step is the production of methyl radicals by electron impact (Equation 2.6).

$$\mathrm{CH_4 + e \longrightarrow e + CH_3^{\cdot} + H^{\cdot}} \tag{2.6}$$

The electron energy varies by the type of discharge, and thus the products also vary. For instance, the reaction chemistry of a pulsed discharge is different from a continuous DBD discharge [75]. At low energies the main radical produced is CH_3 and H which polymerize to form C_2H_6 and H_2. However, at higher energies ($\geq$ 9 eV), the electron impact can produce C, CH, and CH_2 radicals as well, giving rise to a greater variety of products (Figure 2.5) [76].

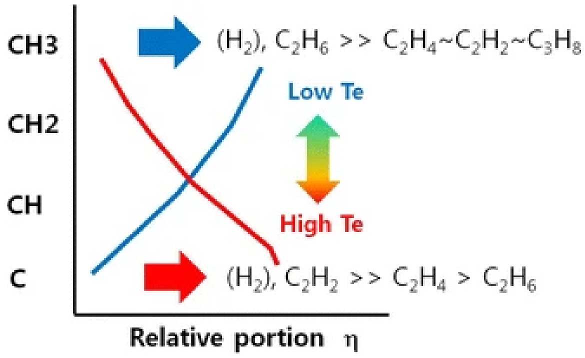

Figure 2.5: Diagram showing comparison of reaction products in CH_4 decomposition with high-energy electrons and low-energy electrons. Primary radicals and final products are compared, has been adapted from [72]

Reforming reactions which are generally accompanied by CO_2 (dry reforming) or H_2O

(steam reforming) can alter the reaction path. C_2H_2 is found to be the most abundant product due to its ability to quickly oxidize, provided there is no quenching/cooling effect. In some cases, for pulsed discharges, the ethylene can be obtained as the abundant product, without getting oxidized to acetylene, owing to its low thermal effect [77]. The dehydrogenation reactions occur at a time scale of 10^{-5} to 10^{-3} seconds, and it is hard to obtain a cooling effect without special provisions in the reactor. Although CO_2 and H_2O favor lower HC formation, it has been observed that the use of H_2 as an additive can aid in the formation of higher HCs [78].

Weakly Exothermic Reactions

These reactions are usually associated with partial oxidation of hydrocarbons, with the heat of reaction being much less than the heat of combustion. For instance, in CH_4 the heat of combustion is -820 kJ/mol, whereas the heat of partial oxidation is -36 kJ/mol [79]. This makes the plasma-induced species to survive for a longer time. In this kind, thermochemistry and plasma chemistry are strongly interactive. There are two ways to supply heat to the system; by increasing ratio of fuel/oxidant or by increasing the electric power. The additional electric power is used as thermal energy, and provides modified conditions for excited gas molecules. The degree of "warmness" is determined by the heat transfer efficiency and possible cooling/quenching.

For conditions without cooling, the degree of "warmness" determines if the plasma chemistry can remain discernible throughout the reaction. The results of Lee et al. [80] provide important information to understand the effect of “warmness” in plasma chemistry. The study investigates the C2 products based on the arc length, to understand the kinetics of thermo chemistry and plasma chemistry (Figure 2.6).

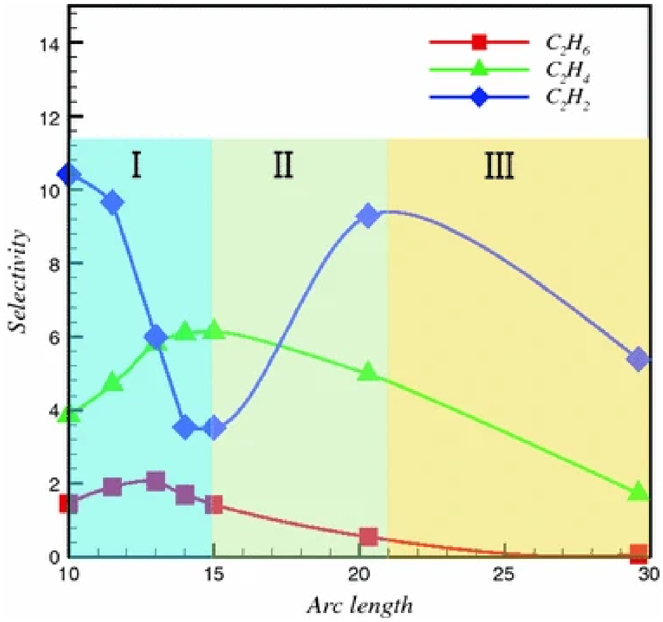

Figure 2.6: Generation of C2 species according to the arc string length in CH_4 partial oxidation processes using rotating arc plasma, has been adapted from [80]

From figure 2.6, it is possible to understand the role of thermochemistry in plasma reactions. The major products were mostly C_2H_4 and C_2H_2 due to the lower electron energy. As the arc length increases, the kinetic source of C_2H_2 changes from hydrogenation to dehydrogenation [81]. With increasing temperature, the voltage requirements for breakdown also get lower, affecting the reaction pathway. Although the reaction is not thermal but weak thermal dehydrogenation results in the formation of more C_2H_6 and

C_2H_4 products compared to C_2H_2. However, at a very high arc length, H abstraction is increased to a state that the formation of C2 products is diminished, with H_2 as the major product [82]. The reaction at these conditions becomes thermally driven and does not give any information on the plasma chemistry.

For conditions with excessive cooling/quenching, the reaction pathway is altered due to suppressed thermal activation. The investigation of Nozaki et al. [83] using a DBD-reactor for partial oxidation sheds some light on this process. In their experiments, the most abundant radical was CH_3 with a source of O radicals to produce CH_3O radicals. The low-temperature oxidation was then possible by cooling, resulting not in the kinetic path $CH_3O \longrightarrow CH_2O$ but $CH_3O \longrightarrow CH_3OH$, by Equation 2.7.

$$CH_3O + CH_4 \rightarrow CH_3OH + CH_3 \tag{2.7}$$

This partial oxidation process (Figure 2.7) can be termed intermittent oxidation. At even

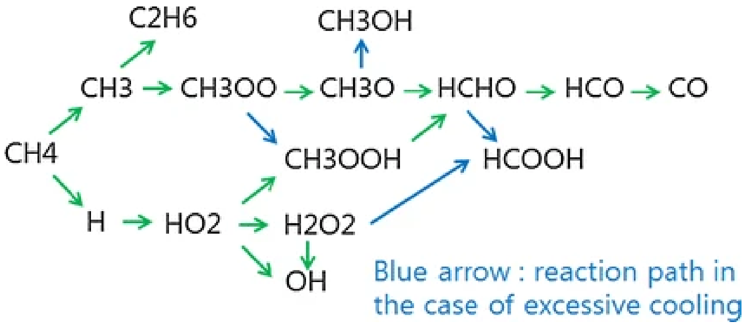

Figure 2.7: Schematic kinetic diagram of CH_4 partial oxidation process with excessive cooling, has been adapted from [84]

lower temperatures of 5 °C, the oxidation process produces oxygenated species as intermediates of final products such as CH_3OOH, $HCOOH$, and CH_3OH [84]. It can thus be expected, that a further increase in electron energy will produce more CH_2 and CH radicals giving rise to higher amounts of C_2H_4 and C_2H_5OH.

2.2.2 Literature review on non-thermal plasma fuel reforming

In the past decade, a lot of attention has been given to the plasma reforming of fuels. In particular, methane, methanol, and ethanol have been studied for H_2 and/or syngas production. Hydrocarbons have also been studied for plasma-reforming. Table 2.3 provides a summary of all the recent studies conducted in this regard.

Table 2.3: A list of recent non-thermal plasma fuel reforming studies

Discharge	**System**	**Substrate**	**Gas**	**Voltage**	**Objective**	**Ref.**
Atmospheric pressure plasma jet	multi-pin glow	CH_4	N_2	5-10 kV	production of H_2, C_2H_2, C_2H_4, C_2H_6	[85]
DBD	continuous flow	CH_4	-	6-12 kV, 0.5-1 MHz	production of H_2	[86]
GAD	continuous flow	CH_3OH	-	-	production of H_2, CO	[87]
Pin-to-plate	in-liquid, batch	CH_3OH	-	200 W, 27.12 MHz	production of H_2	[88]

Microwave	in-liquid, continuous	C_2H_5OH	N_2/Ar	2 kW, 2.45 GHz	production of H_2, C_2H_2, C_2H_4, C_2H_6	[89]
DC pulsed corona	Point-to-plate, continuous flow	C_2H_5OH + gasoline	-	4-5 kV, 8 kpps	production of H_2, C2 HCs	[90]
DBD	in-liquid, continuous	H_2O + C_2H_5OH	-	10-17 W	production of H_2, CO, C2 HCs	[91]
GAD	over-liquid	n-dodecane + H_2O	N_2	10 kV, 50 Hz	production of H_2, C2 HCs	[92]
DBD	continuous flow	n-pentane	CH_4 + CO_2 / N_2 + Ar	1-20 kV, 1-10 kHz	production of H_2, C1-C4 HCs	[93]
continuous DC	tip-cylinder, continuous	n-octane	-	20 W	H_2O/C ratio	[94]
Nanosecond pulsed	nozzle to plate, in-liquid batch	n-dodecane	Ar, CH_4, CO_2	10-12 kV, 4.6 kHz	production of H_2, CO and gasoline ranged fuels (C5-C11)	[95]
Rotating spark gap pulsed power	pin-to-plate, in-liquid batch	Ethanol, Hexadecane, Iso-octane	N_2	20 kV, 240 Hz	production of gas-phase products	[96]

Rotating spark gap pulsed plasma	in-liquid, batch	2,2,4-Trimethylpentane, hexadecane, tridecane, diesel fuel	-	8 kV, 240 Hz	production of H_2 and lower gas fuels	[97]
pulsed spark discharge	in-liquid	gasoline, kerosene, diesel, CH_4	-	10 kV, 100 Hz	production of H_2 and gaseous fuels	[98]
DBD	continuous flow	n-hexadecane	CH_4	0-12 kV, 32 kHz	production of C6-C15 compounds	[99]
DBD	continuous flow	n-hexadecane	$CH_4 + Ar$	9 kV, 18 kHz	production of C1-C15 HCs	[100]
GAD	continuous flow	gasoline	$H_2O + Air$	2.5-5 kV, 50 Hz	calculating efficiency analogous to steam and autothermal reforming	[101]
Microwave jet	over-liquid	n-heptane	Argon	200 W	production of H_2 and C2 products	[8]
Multiphase pulsed plasma	over-liquid	n-hexadecane	$CH_4 + H_2$	40 kV, 10-15 Hz	Production of H_2 and C2-C18 products	[7]

2.2.3 Cost effectiveness of NTP reactors

In a chemical process design using plasma, the following should be considered. First, the degree of thermal activation should be clarified, i.e., the relative contributions of plasma-chemistry and thermochemistry. This understanding will give us an idea of which regime is relevant to the reaction. If plasma chemistry is significant or is effective in the overall reaction, the next step would be to determine the strength of the plasma-chemical reaction. The reduced electric field and SEI can be the indicators. These steps will determine the relative proportions of primary radicals and the relative contributions of diverse hydrogenation and dehydrogenation reactions. Finally, possible quenching or cooling should be considered. The final product can then be estimated. Evaluation of the process should be performed on the basis of the regime relevant to the process [72].

Chapter 3

Plasma synthesis of chemicals from liquid organic compounds

3.1 Preface

This chapter presents the main experimental work carried out, which has been accepted at the journal, *ACS Sustainable Chemistry & Engineering.* The manuscript, entitled *"Plasma-chemical synthesis of valuable fuels and chemicals from n-hexane and its mixtures with methanol and ethanol"*, introduces an NTP reactor, which could simultaneously synthesize H_2 and/or syngas, crack heavy oils, and produce more complex liquid chemicals. The plasma chemistry has also been discussed in the manuscript, to understand the possible reaction pathway. The first author, Avishek Banerjee, is responsible for the experimental design, reactor construction, idea conception, data analysis, and manuscript preparation (original and final draft). The second author, Andrew Golsztajn, supported for setting up analytical methods, and assisted in using analytical instruments and data. The corresponding author, Prof. Pierre-Luc Girard-Lauriault, guided in the idea conceptualization, supervision, funding support, and manuscript editing.

Plasma-chemical synthesis of valuable fuels and chemicals from n-hexane and its mixtures with methanol and ethanol

Avishek Banerjee, Andrew Golstajzn, Pierre-Luc Girard-Lauriault*

Plasma Chemical Processing Lab, Department of Chemical Engineering, McGill University, 3610 Rue University, Montreal, QC, H3A 0C5, Canada

Keywords: non-thermal plasma, organic synthesis, hydrogen, fuel reforming, plasma chemistry, sustainable technology, fuels and chemicals

Abstract

Among several emerging technologies that are focused on finding sustainable routes of reforming heavy oils and/or alcohols into valuable fuels and complex chemicals, non-thermal plasma shows promise both due to its non-equilibrium nature and its ability to use intermittent renewable electricity. In this work, we investigate its interaction with organic compounds as a “green” process for simultaneously synthesizing hydrogen, cracking heavy oils, and producing more valuable, complex chemicals. A pin-to-plate microsecond pulsed argon plasma was used at temperatures of 20°C, 0°C, and -20°C. Using 390 kJ/kg of specific energy input we were able to achieve a conversion efficiency of 771.4 mmol/kWh for the treatment of hexane-ethanol mixture at 0 °C. It is concluded that the production of H_2

and other lower fuels (gas hydrocarbons) can be increased by the addition of alcohols in our reforming processes. At 0°C, the production efficiency and selectivity of gas products were found to be higher compared to other temperatures. A Low temperature of -20°C showed the highest production efficiency for liquid products. Product formation was observed to mainly undergo dissociation and dehydrogenation, whose reaction pathway is also discussed.

3.2 Introduction

The reformation of fuels has garnered increased interest as the world is looking to move towards cleaner forms of energy. Conventional methods of thermal reforming are energy-intensive with high CO_2 emissions and are often accompanied by catalysts [102, 103]. Emerging substitutes include radiation processing [3, 4], biochemical conversion [5], and photochemical conversion [6], but their high temperature/dosage requirement with low power density limits their industrial implementation. Therefore, the need for a more economical and environment-friendly alternative has brought non-thermal plasma (NTP) technology to the forefront of ongoing research efforts. It can operate under ambient conditions with an energy cost of 1-3 eV/molecule, and its non-equilibrium nature enables thermodynamically unfavorable reactions to proceed at low temperatures [9]. In addition, NTP provides an efficient and flexible way of converting intermittent renewable electricity (solar or wind) into chemical energy and in turn can mitigate its storage problems [10]. Recent investigations on the role of gas temperature and energetic electrons in plasma chemistry have further opened new paths of exploration involving reforming processes [8].

NTP has been studied various carbon sources, but it has been limited mainly to the formation of high value lower fuels (H2, CO, and C1-C5). Discharges on gas-phase methane [86, 104], methanol [87, 88], ethanol [89–91] and hydrocarbons, like n-pentane, n-dodecane, and n-octane, were studied extensively for the synthesis of hydrogen and other lower hydrocarbon fuels [92–94]. They involve evaporation costs, limiting the ability to accommodate various feedstocks. Use of liquid organic compounds is thus promising and a few related studies exist with corona discharge [95–98], dielectric barrier discharge [99, 100], and gliding arc discharge [101], where the discharges are directly generated inside the liquid medium. The problem with such discharges is the high density of liquid compared to gases making the breakdown electric field higher [9, 105]. Therefore, the suitable alternative is gas discharges over liquids which can form a broader range of products both at the gas-phase and liquid-phase and consequently provides a vast field of exploration.

To our knowledge, very few gas discharge over liquid studies were recently conducted with n-dodecane by Whitehead and Prantsidou [106], with n-heptane by Hamdan et al. [8], and with hexadecane by Wang et al. [7]. Whitehead and Prantsidou observed 10% conversion into gas products in their gliding arc reactor. Hamdan et al. used a microwave plasma jet for n-heptane reforming and found more than 40% selectivity for C_2H_4. Wang et al. observed

9.36% hexadecane conversion in their pulsed plasma reactor. However, in all the studies, very little attention has been provided to understand the plasma-chemistry of the system. The experiments were not temperature controlled, liquid products were not analyzed, and microwave plasma which has been studied to have a thermal effect [107] was used by Hamdan et. al.. Gas discharges over liquids initiate very complex reactions as when the gas in the discharge region ionizes, it can form reactive species in the gas phase or can penetrate the bulk of the liquid. This lead to the formation of valuable compounds in both phase through complex mechanisms. Thus, there remains a vast knowledge gap in understanding these mechanisms for which extended research is still required.

Our aim is to use both hydrocarbon and alcohols at once with NTP as a technology that can simultaneously produce H_2 (or syngas), help in cracking of heavy oils, as well as produce complex and valuable liquid chemicals. This paper focuses on gas discharge over liquid organic compounds to control/induce certain radical reactions for specific syntheses by (a) reaching low temperatures down to -20 °C such that thermal energy has the least effect on product formation and vapor pressure of the liquids, and (b) using n-hexane as a model hydrocarbon along with liquid alcohols to alter the selectivity of the products formed. Addition of alcohols further reduces the dielectric permittivity of the mixture and drastically reduces the operating voltage. Methanol and ethanol were chosen as they are the simplest alcohols and are considered valuable in the renewable energy sector with a a higher-octane rating and lower emissions. To achieve the stated objectives, a pin-to-plate pulsed dielectric barrier discharge was used, which can operate at lower discharge temperatures compared to other kinds of discharges. Argon was used as the discharge gas to facilitate clean formation of products. The gas and liquid products were closely monitored to gain insights into the chemistry of plasma syntheses. After identifying the common products formed from the different experiments, a possible chemical pathway was established by which the reactions can occur. The performance of our proposed reactor is also compared to similar works to obtain the viability of our solution.

3.3 Materials and Methods

Figure 3.1 shows a schematic of a pin-to-plate microsecond pulsed plasma reactor system. A benchtop jacketed reaction vessel of 500 mL was used for the experiments and stainless-steel (S.S) electrodes were used for the pin-to-plate discharge. The ground electrode with a glass dielectric barrier was submerged in the liquid and the high voltage electrode was in the gas phase both of which are approximately 2 mm on each side of the surface of the liquid. A microsecond pulsed dielectric barrier discharge (DBD) was obtained as a result. A constant gap was maintained across all the experiments such that the breakdown voltages are independent of the discharge gap. The capacitance of the system was measured to be 12 pF. A high voltage pulsed power supply at a frequency of 6 kHz was used, corresponding to output voltages in the range of 14–24 kV. The discharge voltage and the currents were measured using a Tektronix P650A voltage probe and a Pearson 411 current probe respectively, connected to an electronic oscilloscope (Picoscope 2408B). A recirculating chiller was used to control the temperature of the reactor. The experiments were performed at -20 °C, 0 °C, and 20 °C. Argon gas was bubbled from the bottom of the reactor with a flowrate of 0.24 L/min to purge the headspace and to facilitate mixing in the liquid by the movement of the bulk liquid molecules. Another advantage of bubbling argon is that at a low temperature of -20 °C, where the vapor pressure becomes very low, reducing volatility by a great extent, the liquids can form a film over the bubbles and reach the plasma discharge region to give gas products. Hexane-alcohol mixtures supplied higher power and energy to the system followed by the alcohols, whereas hexane provided the least power and energy (Figure 3.13, section 3.6.2). Hydrocarbon liquids used in our study comprised of n-hexane ($\geq$ 99%), methanol ($\geq$ 99.9%), and ethanol (anhydrous). A volume of 100 mL was used for all the experiments and was treated either in their pure form or in a 1:1 mixture. The treatment time was fixed to 20 mins across all the experiments.

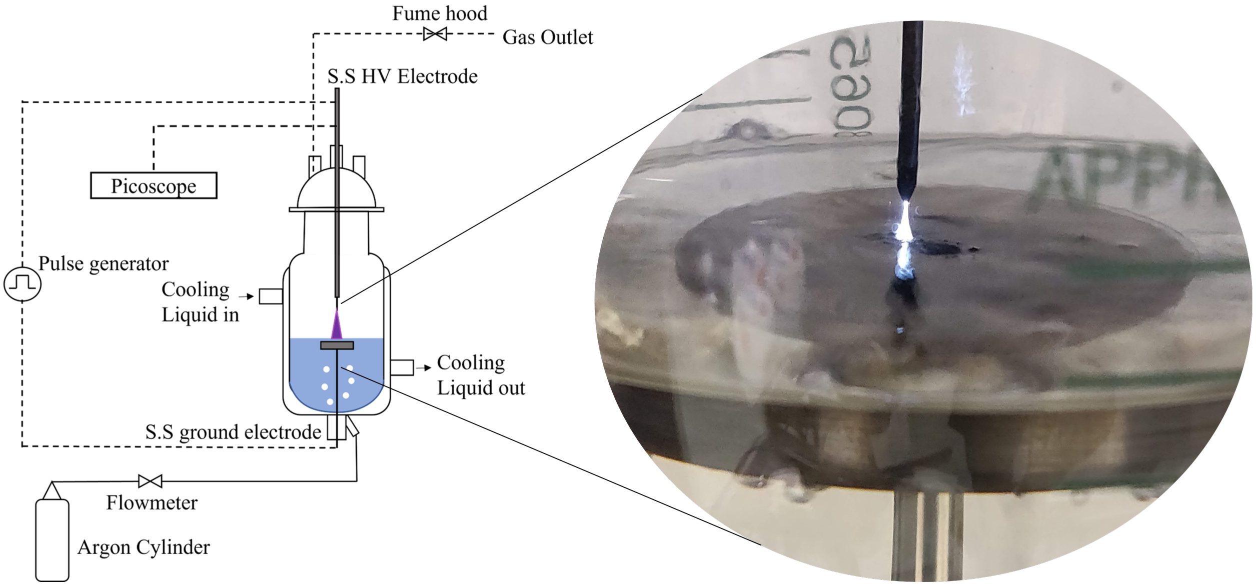

Figure 3.1: Schematic and visual representation of the pin-to-plate microsecond pulse DBD plasma reactor used for reforming reactions

At the start of the 20th min, the gas samples were collected into a Tedlar bag for 1 min. Liquid samples were collected at the end of 20 mins into GC amber vials. The product characterization was done using gas chromatography-thermal conductivity detector (GC-TCD) for the gas samples (section 3.6.3, Figure 3.14) and gas chromatography-mass spectrometry (GC-MS) for the liquid samples (section 3.6.5, Figure 3.17). The production efficiency of gas products, η_g (mmol/kWh), production efficiency of liquid products, η_l (g/kWh), relative yield %, and selectivity % of the acquired data were obtained through standard methods widely known and found in literature [8, 95].

3.4 Results and Discussions

3.4.1 Gas-phase product analysis of different HC mixtures at room temperature

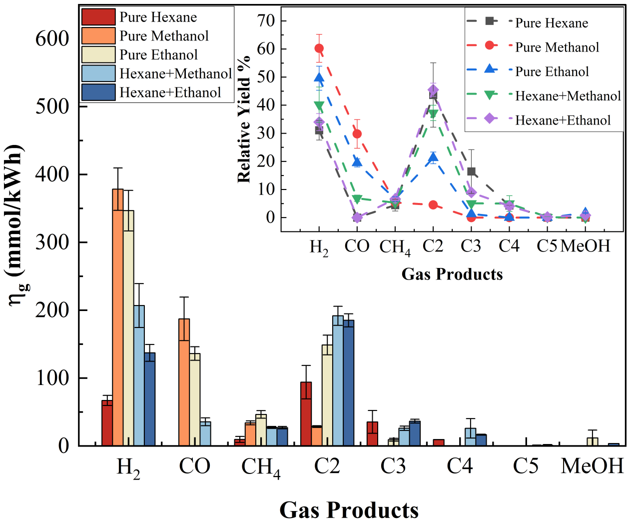

Figure 3.2: production efficiency (mmol/kWh) and relative yield % of different gas phase products when pure hexane, pure methanol, pure ethanol, hexane+methanol, and hexane+ethanol is treated with microsecond pulsed plasma

To understand the reaction chemistry, we first investigated the reformation of hexane and its mixture with methanol and ethanol at 20 °C. Figure 3.2 shows the production efficiency and relative yield % of H_2, CO, and HCs from different plasma treated liquid mixtures. The major component formed was H_2 followed by CO and HCs (mainly C1-C4 consisting of methane, ethane, ethylene, acetylene, propylene, propadiene, butane, isobutane, butadiene). It should be noted that other than H_2, CO and HC gas products, negligible amounts of methanol were formed from hexane-ethanol and pure ethanol treatments (Figure 3.2). The H_2 relative yield was observed to be the lowest for pure hexane at 31.1% and the highest for pure methanol treatments at 60.2%. Although the α-C-H bond in ethanol is weaker than in methanol, the higher vapor pressure of methanol allows for more molecules to be present in the plasma discharge which, in turn, allows for higher production of H_2 [108, 109]. Similarly, H_2 production efficiency was the highest from pure methanol at 378.4 mmol/kWh and pure ethanol at 346.6 mmol/kWh. The H_2 formation is mainly carried out in the vapor phase and there is very little chance of H_2 molecules escaping from the liquid, which further demonstrates that the vapor pressure of the liquid plays a crucial role [7]. It was slightly lower for hexane-methanol and hexane-ethanol mixtures at 206.8, 137 mmol/kWh but still higher than pure hexane. It can be concluded that the addition of alcohols to heavy oils can help increase the production of H_2. The production efficiency of lighter hydrocarbons, mainly the C2 products, were found to be the highest for hexane-methanol and hexane-ethanol mixtures at 191.7 and 185 mmol/kWh with a relative yield of 37.3% and 45.5% respectively. As the reactions are mainly driven by dissociation, the presence of a high number of carbon atoms in hexane and the easy dissociation of methanol/ethanol contribute to the higher production of C2 hydrocarbons [110]. It also conforms that the production efficiency of C2 hydrocarbons from methanol is very low as it consists of 1 C atom producing H_2 and CO as the main component [111].

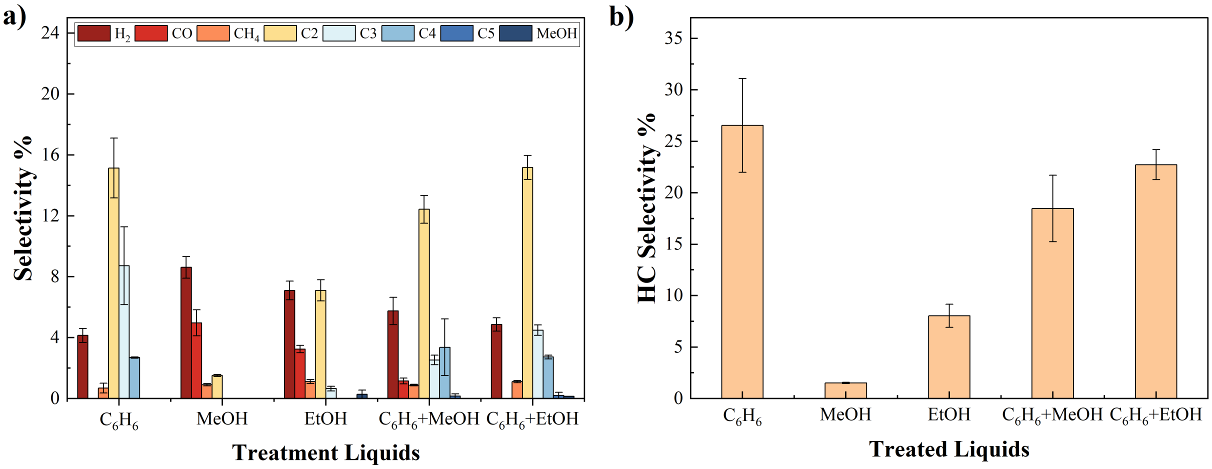

Figure 3.3: (a) Selectivity of different gas products for different treated liquids at 20 °C (b) HC Selectivity (negligible amounts of methanol was not considered) for different treated liquids

Figure 3.3 shows the selectivity of different products at 20 °C and the total HC (C1-C5) selectivity. The H_2 selectivity was observed to be the highest in methanol at 8.6%, followed by ethanol at 7.1%. The selectivity of H_2 decreased with alcohol mixtures (5.7% for hexane-methanol and 4.9% for hexane-ethanol) due to the favoring production of C2, C3, and C4 hydrocarbons. The selectivity of C2-C5 hydrocarbons was found to be higher in pure hexane, hexane-methanol, and hexane-ethanol mixtures at 26.5%, 18.5%, and 22.7%. The higher selectivity of HCs attributes to the fact that the C-C threshold bond energy is lower than that of the C-H bond giving rise to more $C_6H_{11}\bullet$ radicals compared to $H\bullet$ radicals. The selectivity for CH_4 almost remained unchanged with different treatment liquids [112]. Thus, it can be possible to control the selectivity of the products using specific liquid composition as it produces different active species in the form of radicals, ions, and/or excited molecules.

3.4.2 Effect of reactor temperature on gas-phase products

Figure 3.4 shows the production efficiency of H_2 and HCs (C2-C5) with temperature. It was observed that the production efficiency of both H_2 and HCs was higher at 0 °C for all the treated liquids. H_2 production efficiency was the highest for methanol, 429.9 mmol/kWh, at 0 °C, followed by ethanol and hexane-alcohol mixtures. The H_2/CO production ratio was between 2 and 2.8 in methanol and ethanol (section 3.6.4, Figure 3.16). At 0 °C, the gas HC production efficiency for hexane-ethanol and hexane-methanol mixture at 419.1 mmol/kWh and 333.6 mmol/kWh, respectively, were found to be higher .

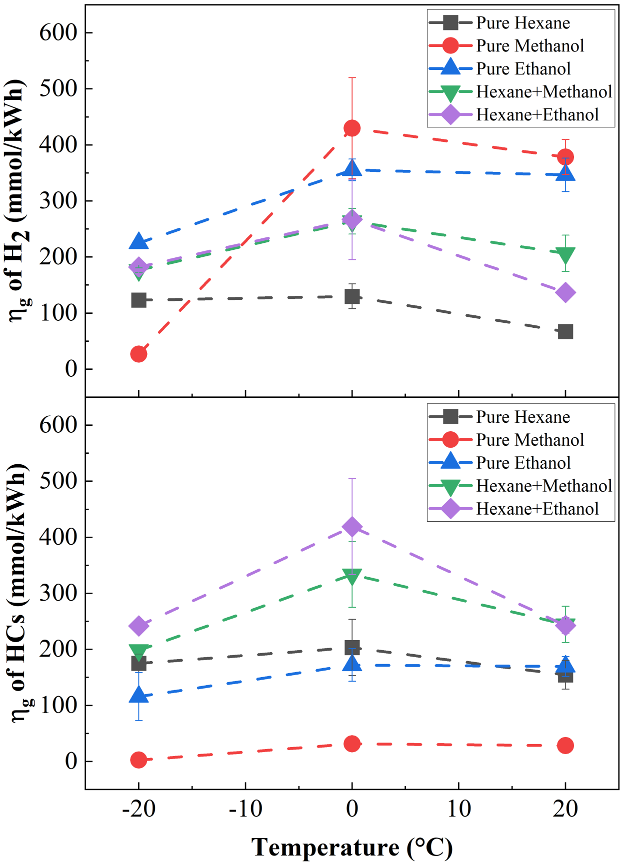

Figure 3.4: Production efficiency of H2 and gas-phase HCs (negligible amounts of methanol was not considered) with temperature for different hydrocarbon liquid mixtures

The selectivity of H_2, CO, and HCs all varied with temperature. For HCs, only C2 and C3 selectivity were plotted in Figure 3.5 as they showed significant selectivity compared to C4 and C5. The selectivity of H_2 was found to be higher in methanol and ethanol with the highest selectivity of 9.4% for methanol at 0 °C. The HC selectivity was however found to be higher for hexane and hexane-alcohol mixtures, for the possible reasons stated above. The highest selectivity for C2 and C3 reached 15.2% and 8.7% respectively, for hexane-methanol and hexane treated liquids at 20 °C. It may indicate that the product selectivity depends on the reactor temperature, as it can significantly alter the reaction pathway. A high amount of gas products was produced at higher temperatures owing to the higher vapor pressure of the liquid organics at 20 °C, which could be a factor in the higher selectivity. At low temperatures, the gas product formation decreases but the operating voltages lower significantly, giving a higher production efficiency. So, a higher reaction temperature may favor product selectivity at the cost of production efficiency for pure n-hexane experiments. It is the same for liquid products from methanol and ethanol in liquid products. However, for gas products, we hypothesize that since the vapor pressure of methanol and ethanol is lower than hexane at low temperatures, and they already have a low number of carbon atoms, they do not produce enough hydrocarbons. However, the original trend still follows for H_2 gas.

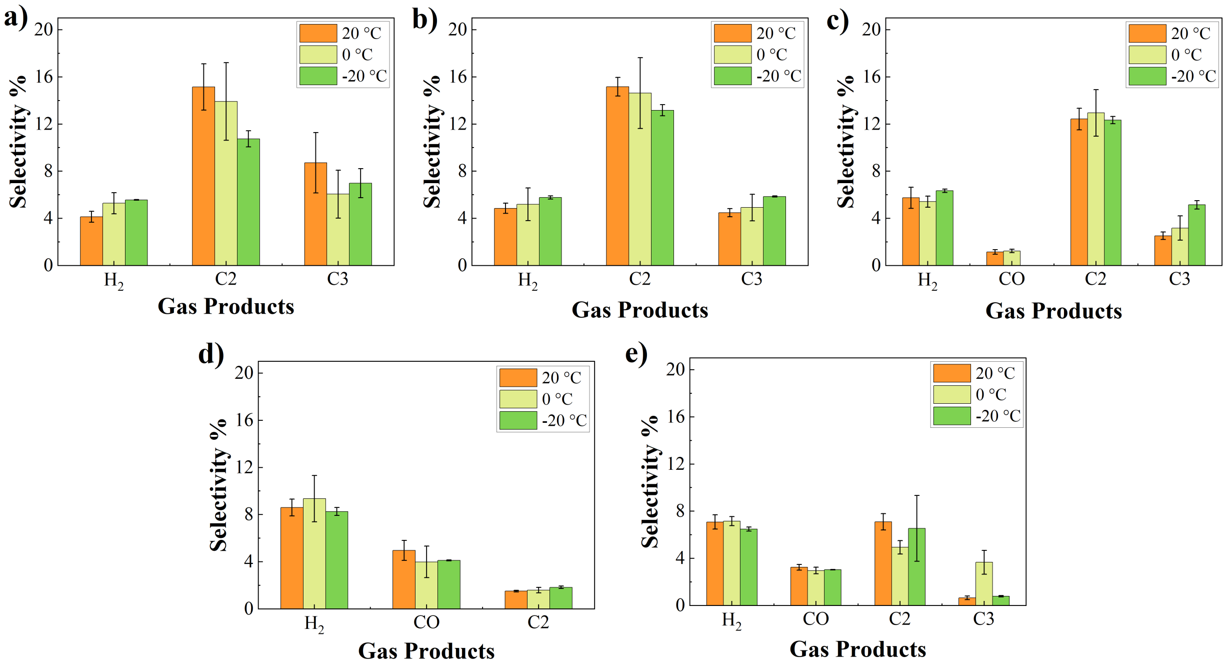

Figure 3.5: Selectivity % of different gas products formed from (a) hexane (b) hexane+methanol (c) hexane+ethanol (d) methanol and (e) ethanol at different temperatures

3.4.3 Liquid-phase product analysis of different HC mixtures at room temperature

The liquid products from the treatment of different liquid mixtures were presented, except for the pure alcohols. The only liquid products formed from methanol treatment were ethylene glycol and from ethanol treatment were C3-C5 alcohols (Figure 3.19). Figure 3.6 shows the production efficiency, relative yield%, and selectivity% of liquid products.

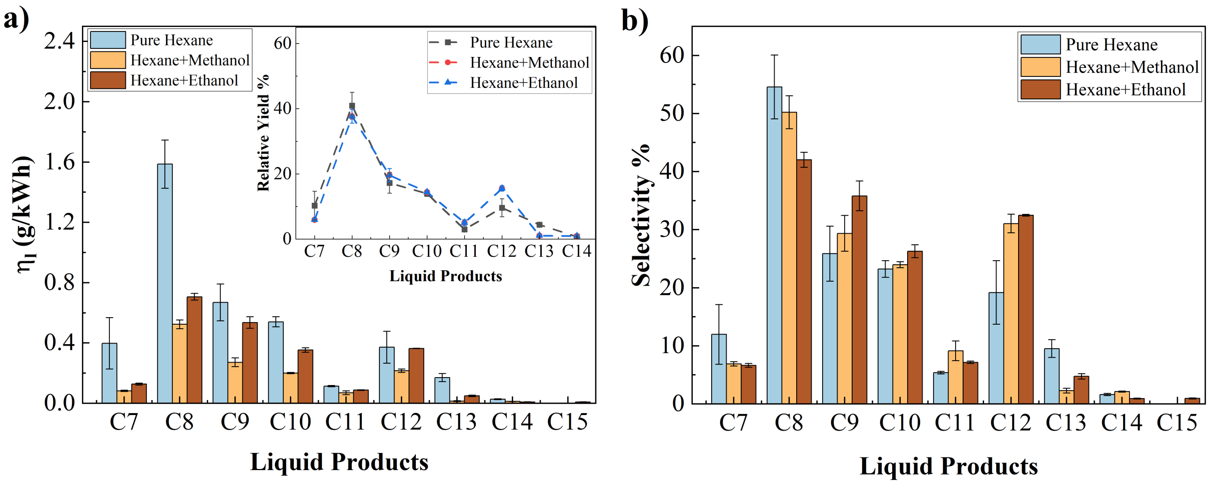

Figure 3.6: (a) production efficiency and relative yield (b) selectivity of liquid products formed from pure hexane, hexane+methanol, and hexane+ethanol mixture at 20 °C.

Treatment of pure hexane gave the maximum efficiency of liquid products. As the carbon number increased from C8 to C15, we observed the production efficiency decreasing. C8 was observed to be the highest followed by C9, C10, and C12 at 1.6, 0.7, 0.5, and 0.4 g/kWh with a relative yield of 40.9%, 17.3%, 13.9%, and 9.6% respectively. Some of the C7 products could have coincided with the solvent front of the GC-MS owing to the lower amounts recorded in our study. The high amounts of C12 products compared to C11 products can be due to some form of dimerization that takes place in our plasma chemical reactions. In hexane-alcohol mixtures, liquid products were formed at a lower efficiency which can be related to the quenching effect from the OH groups in the alcohols. It was previously reported that although OH groups facilitate oxidation reactions, they also prevent alkyl-alkyl recombination. Whereas CH3 • and H • radicals in the liquid facilitate the formation of lower

HCs (gas products) [95]. The relative yield of all the liquid products remained almost the same irrespective of the liquid used for treatment, with the hexane-alcohol mixtures almost coinciding with each other. Although a high selectivity value was observed for C8 with pure hexane at 54.6%, selectivity values of C9, C10, and C12 were higher for hexane-ethanol mixture at 35.8%, 26.3%, and 32.5% respectively.

3.4.4 Effect of reactor temperature on liquid-phase products

The reactor temperature controls the gas dynamics inside the reactor and can affect the production efficiency and selectivity of the liquid products. Figure 3.7 shows the production efficiency and relative yield% of liquid products with temperature.

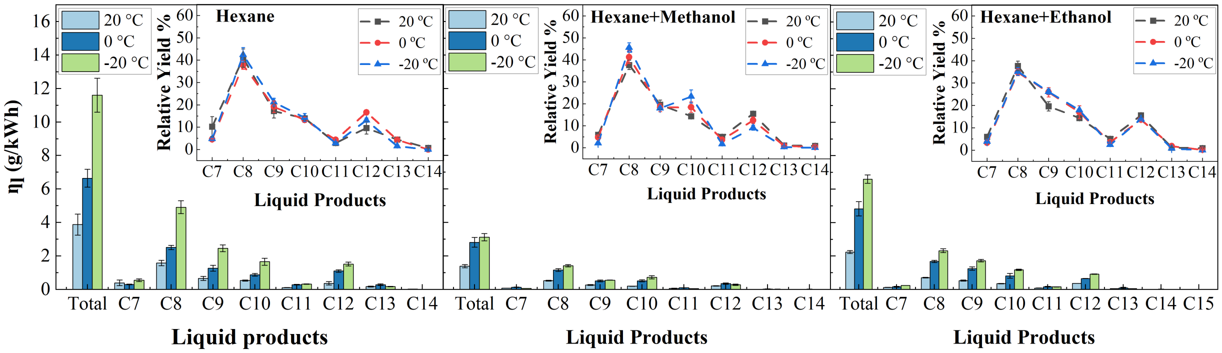

Figure 3.7: Production efficiency of total HCs and products from each carbon family, and relative yield % of each carbon family as part of liquid products

We observed that the production efficiency of all the liquid products showed an increasing trend with lower temperatures. The highest efficiency of liquid products, 11.6 g/kWh, was observed with the treatment of hexane at -20 °C. The relative yield of the products did not change much with temperature, as can be seen from Figure 3.7. The higher production efficiency can be attributed to the lower breakdown voltages required for plasma discharge in an argon-dominated environment. Furthermore, the current observed at lower temperatures is much higher as seen in (Figure 3.13c). and so, there are more energetic electrons that can attack multiple sites of the liquid hydrocarbon to form new products. The selectivity was also studied across the different temperatures for hexane and hexane-alcohol mixtures, but it did not vary significantly (section 3.6.6, Figure 3.21).

3.4.5 Reaction pathway

The main chemical reactions are driven by the radicalization of the various hydrocarbon reactants that we used in our experiments. Different products are formed due to the presence of multiple sites for the original radical to attack which leads to thermodynamically unfavorable reaction pathways [12]. While the gas products remained almost the same across all sets of experiments, the liquid products varied significantly with different starting reactants.

In the system, for hexane treatment, the highly energetic electrons can break the monomer from the C1-C2, C2-C3 or the C3-C3 site. The bond dissociation may be mainly driven by hydrogen abstraction followed by the formation of methyl $CH_3\bullet$, ethyl $C_2H_5\bullet$, and propyl $C_3H_7\bullet$ radicals. These radicals may further react to form methane, acetylene, ethylene, ethane, propylene, and propane, all of which are observed in our gas-phase products. The presence of C4 and C5 compounds in the gas phase is also an indication of the formation of butyl $C_4H_9\bullet$ and pentyl $C_5H_{11}\bullet$ radicals, however, due to their low amounts, they could not be significantly identified across all experiments [113]. A similar pathway is followed by pure methanol and ethanol liquids as well. The breakdown products of methanol would be methyl and OH radicals and for ethanol would be methyl, ethyl, and OH radicals which recombine among themselves to form different products. Figure 3.8. proposes a possible reaction pathway for the formation of all the identified gas products.

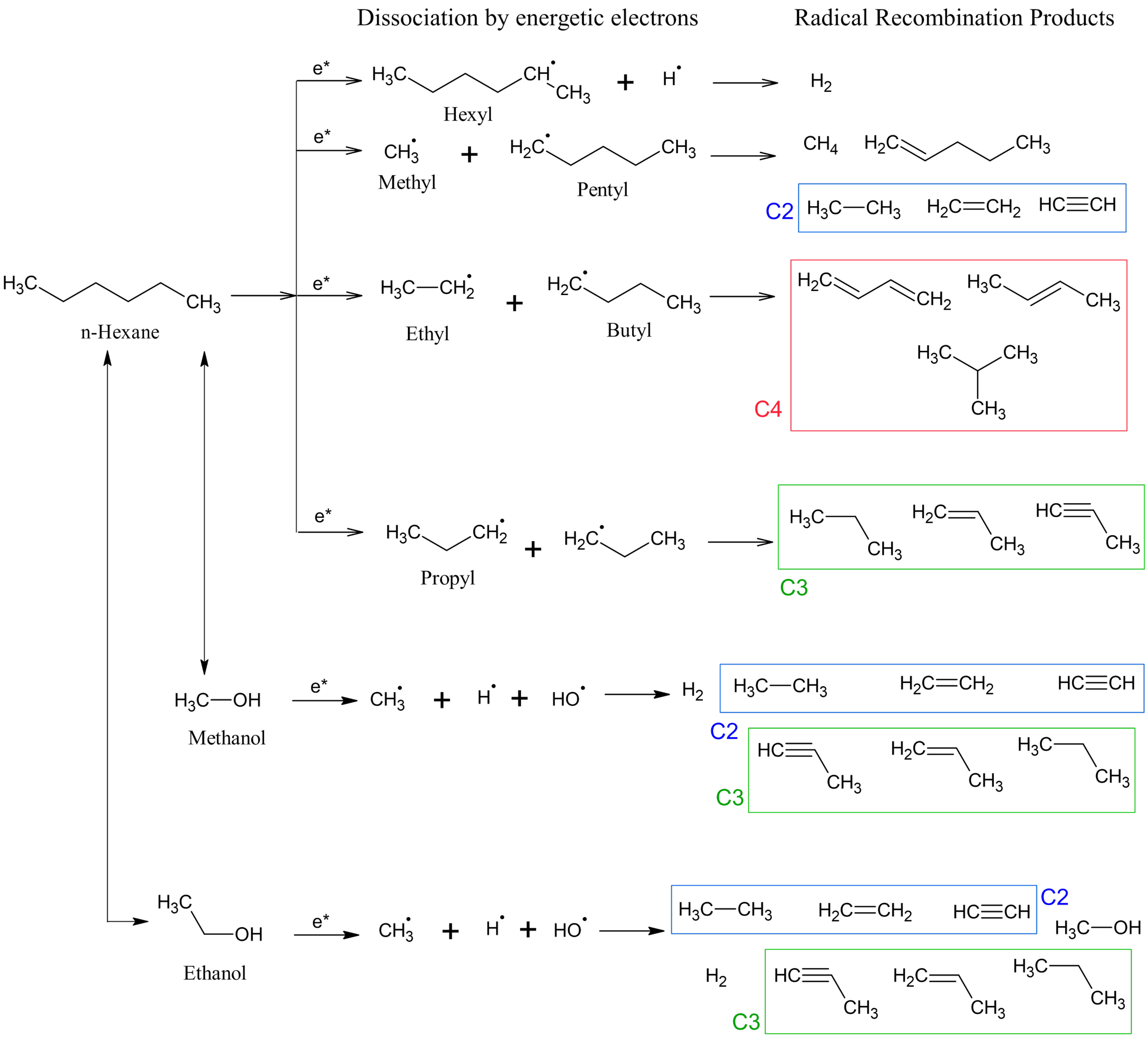

Figure 3.8: Proposed reaction pathway for the formation of identified gas products, blue-C2 products, green-C3 products, red-C4 products.

The higher products formed from hexane and its mixtures with ethanol and methanol are mostly present in the liquid phase, as shown in Figure 3.9. Their formation can be a result of the radicalization of C atoms and bond dissociation. However, the easiest way is by abstraction of hydrogen as it has the lowest activation barrier compared to the higher C-C bond cleavage energy (≈ 40 kcal/mol) which readily forms hexyl radicals. Methanol and ethanol can similarly undergo OH abstraction that form methyl and ethyl radicals respectively. These radicals can then undergo the following reactions (a) recombination with an H to form hexane, (b) conversion to isomers of higher alkanes/alkenes/alkynes, and (c) attaining different oxidation levels through the formation of alcohols, hydroperoxides, and ketones [110].

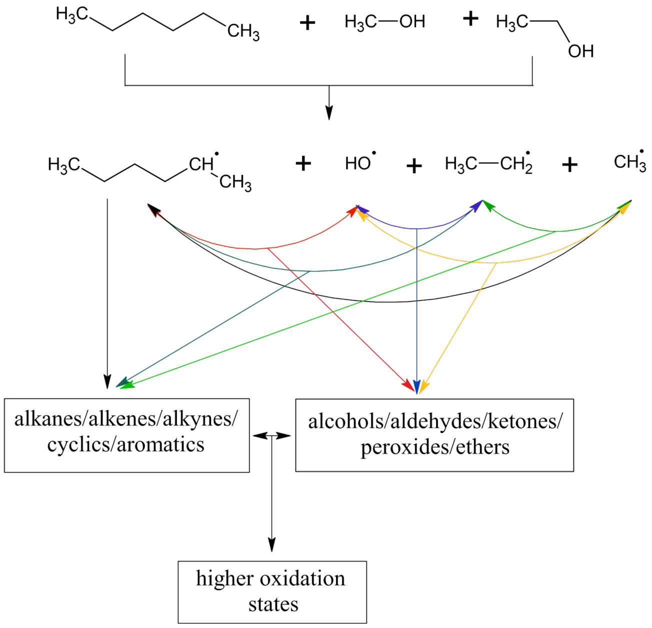

Figure 3.9: Proposed reaction pathway for the formation of liquid products

3.4.6 Performance evaluation

Figure 3.10 shows the conversion efficiency of different hydrocarbon mixtures at different temperatures and a comparison of specific energy (SEI) input with cooling energy. Table 3.1. compares the performance of plasma synthesis of different hydrocarbons for gas discharge over liquids. The conversion efficiency with an SEI of 390 kJ/mol was found to be the highest, 771.4 mmol/kWh, with a corresponding SEI of 390 kJ/kg for hexane-ethanol mixture at 0 °C, which is higher than other studies carried out with noble gases or nitrogen. The energy used for reducing the temperature to 0 °C (between 45.9-49.9 kJ/kg for different liquid mixtures) outweighed the energy required for cooling significantly, as can be seen in Figure 3.10b, but the change was not significant from 0 °C to -20 °C. It should be noted that for hexadecane transformation by Wang et al., CH_4 and H_2 were used, which could facilitate much of the plasma chemical reactions through the gas radicals and does not give us the actual idea of plasma chemistry in the system. Hexane-methanol also showed high efficiency of 716.6 mmol/kWh at 0 °C. It can be concluded that the hexane-alcohol mixtures provide a higher conversion overall predominantly through gas-phase conversion.

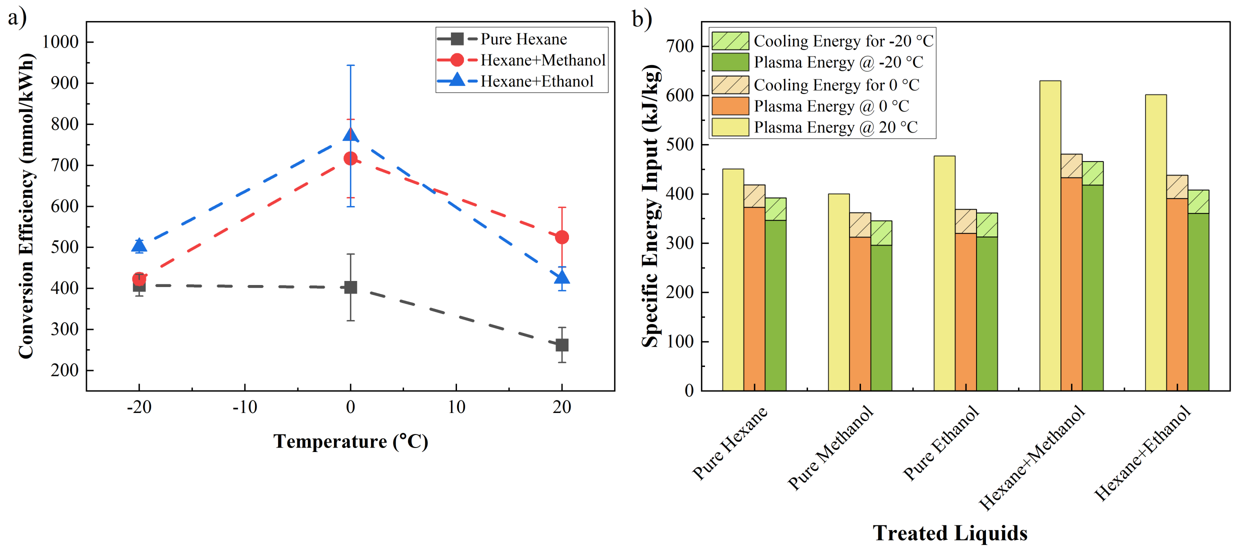

Figure 3.10: (a) Conversion efficiency of pure hexane, hexane+methanol, and hexane+ethanol at different temperatures (b) comparison of specific energy input (plasma energy) with cooling energy consumed

Table 3.1: Comparison of plasma-reforming of gas discharge over liquid organic compounds

Plasma Type	Reactant	Carrier gas	SEI (kJ/kg)	Conversion	References
GAD-Plasma	n-dodecane	N_2/H_2O	17600	300	[95]
Microwave Plasma Jet	n-heptane	Argon	438.6	365	[8]
Multiphase pulsed plasma	hexadecane	90% CH_4 + 10% H_2	500	2894	[7]
DBD microsecond pulsed plasma	n-hexane hexane+methanol hexane+ethanol	Argon	343.6 429 390	407.8 716.6 771.4	Our work

In comparison, current fluid catalytic cracking (FCC) processes require an SEI of more than 5000 kJ/kg at a temperature of 450-550 °C with continuous catalyst regeneration, which also accounts for the second-highest cost after feedstocks [114]. Furthermore, the system operates at ambient conditions and would not require any additional compression for transporting the gas and liquid products. It is a small scale, portable operation with low social and energy costs and can be scaled-up through multiple reactors or by using a multi-pin discharge.

3.5 Conclusions

In this work, we demonstrate plasma reforming of organic compounds, which can be a potential alternative in the fuel processing or biofuel industry. Our SEI is lower than other emerging technologies and similar plasma technologies, providing a conversion efficiency comparable to or more than other studies. Using 390 kJ/kg of SEI (<$1/barrel) [7], we were able to have a conversion efficiency of 771.4 mmol/kWh for the treatment of hexane-ethanol mixture at 0 °C. Pure hexane showed the maximum gas HC selectivity (26.5%), indicating that the addition of alcohols quenches down the formation of HCs, while the highest selectivity of H_2 (9.4%) was observed at 0 °C from methanol. Liquid products showed high production efficiency of C8 products, and it kept on decreasing for higher carbon products. The relative yield of the liquid products remained the same across different experiments. As the temperature was lowered to -20 °C, the production efficiency of the liquid products increased. However, the selectivity of the liquid products remained constant with changing temperature and the highest selectivity was observed for C8 (55.3%) from hexane-methanol treatment. The results are further supported by a detailed analysis of the plasma-chemical reaction pathway that can be induced in the system.

Using renewable electricity, the process was proven to be successful in converting liquid fuels. Although it showed minimal production of CH_4, it did not show any production of

CO_2, which can significantly aid in lowering GHG emissions. It can also be concluded that the production of H_2 and other lower fuels (gas HCs) can be achieved using hydrocarbon-alcohol mixture in our reforming processes. At 0 °C, the production efficiency and selectivity of gas products were found to be higher than other temperatures, which can aid future research focused on increasing energy efficiency with similar processes. H_2 which is a co-product of our proposed technology can be used in hydrotreating or hydrocracking [115]. Future work may focus on the use of different plasma-medium (using different gas mixtures), the effect of gas recycling, addition of catalysts, multi-pin discharge, and/or multiple series reactors to further optimize and scale-up the process.

ACKNOWLEDGEMENT

This work was supported by the Natural Sciences and Engineering Research Council of Canada (NSERC) under Grant NSERC RGPIN-2018-06421 and the Mitacs Globalink Graduate Fellowship. The authors would like to thank Petr Lukes for providing inspiration for a part of the experimental design. We would further like to thank the Analytical Lab officials for granting generous access to its facilities for the use of GC-MS and GC-TCD.

3.6 Supporting information

3.6.1 Materials and equipment used

A benchtop jacketed reaction vessel of 500 mL volume along with a 3-neck vessel lid from Chemglass Life Sciences Inc. was used. As point-to-plane electrode configuration, two stainless steel electrodes were used (both ordered from McMaster-Carr). A stainless-steel disc of diameter 2 inch was polished and fixed above a 5 mm diameter stainless steel rod to act as the ground electrode and a 2 mm stainless steel rod was sharpened at one end to act as the high voltage point electrode (both are multipurpose 304 stainless steel ordered from McMaster-Carr and machined at the Wong Workshop in the Department of Chemical Engineering, McGill University). The electrodes were connected to a G2000 microsecond pulse generator from Redline-Technologies. A Tektronix P650A voltage probe was purchased from Fischer Scientific, and a Pearson 411 current probe was purchased from Pearson Electronics respectively. Picoscope 2408B was used as the electronic oscilloscope and was purchased from Pico Technology. The reactor side drain outlet was connected to a Matheson Flowmeter (E406) for the introduction of Argon gas into the reactor chamber. The jacketed part of the reactor was connected to a recirculating chiller (VWR refrigerated circulator with cooling capacity of 505 W at 20 °C that can go down till -40 °C) to maintain a constant temperature. The reactor system was held with the help of a support stand and a chain clamp. Argon gas of purity 99.99% used was supplied by MEGS (division of Air Liquid). Ethanol anhydrous was purchased chemical engineering store at McGill while n-hexane (≥99%), and methanol (≥99.9%) was purchased from Sigma-Aldrich.

3.6.2 Electrical characteristics

To obtain the electrical curves, a code was developed using MATLAB®. The code used the recorded current (I) and voltage (V) values during the plasma treatment. The electrical parameters were taken at 5 different times: 0, 5, 10, 15, and 20 min after the experiment had started. The calculation was adapted from Rusterholtz's method [116, 117].

To find the capacitance, C, of the system the pulse generator was turned on without plasma activation. The air gap between the two electrodes were increased to achieve this. The displacement current was then measured through the following equation and the capacitance was found to be 12 pF.

$$I_{meas,noplasma} = I_{displacement} = C\frac{dV}{dt} \tag{3.1}$$

The conductive current is the current responsible for the plasma discharge and is calculated as follows.

$$I_{conductive} = I_{meas,plasma} - I_{displacement} \tag{3.2}$$

Figure 3.11. shows a typical V-I waveform for plasma treatment of hydrocarbons. The duration of each pulse was 166.67 µs. A phase shift of 90° was considered in all the

calculations as the power supply is an RC circuit. Figure 3.12. Resembles a circuit diagram of the setup.

The discharge power was calculated from the picoscope data for our analysis. The energy per pulse (E_{pulse}) and discharge power (P) of the system can be calculated as follows

$$E_{pulse} = \int_{0}^{t_{pulse}} V_{meas} \left(I_{meas,plasma} - C\frac{dV}{dt} \right) \, dt \tag{3.3}$$

$$P = E_{pulse} \times frequency \tag{3.4}$$

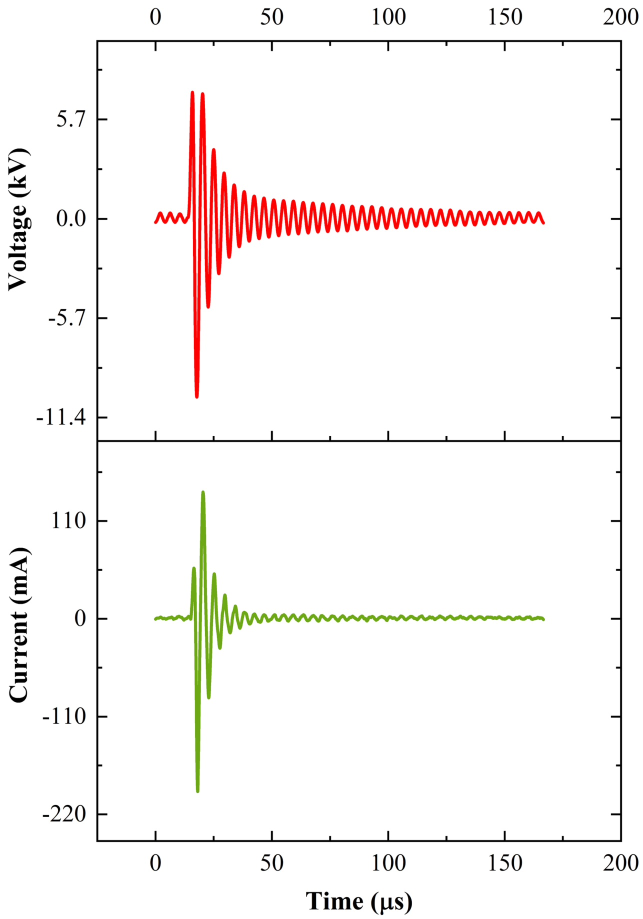

Figure 3.11: Voltage and current waveform with time

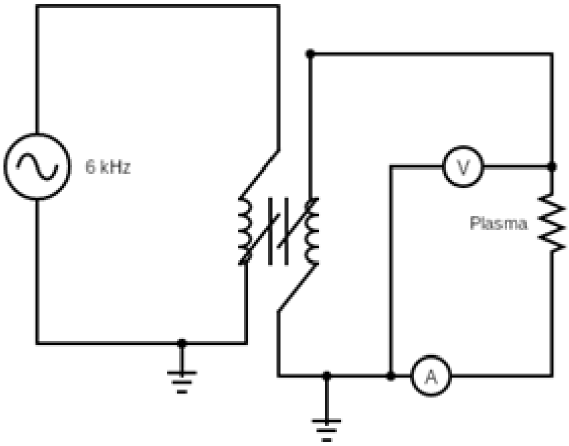

Figure 3.12: Schematic of Electrical Circuit

We investigated the electrical characteristics of the plasma discharge for different liquid mixtures and with different temperatures. Although the applied voltage and frequency were kept constant throughout all the experiments, it was found that the discharge physics was largely affected by the composition of the liquid and reactor temperatures. The dissipated power and energy calculated were found to be higher for the hexane-methanol and hexane-ethanol mixtures as opposed to pure hexane, methanol, and ethanol as shown in Figure 3.13. A correlation was made with vapor pressure (Pv). For hexane-methanol Pv, both were considered miscible due to the constant bubbling of argon gas from the bottom of the reactor that would create perturbations in the liquid and facilitate mixing throughout the plasma discharge.

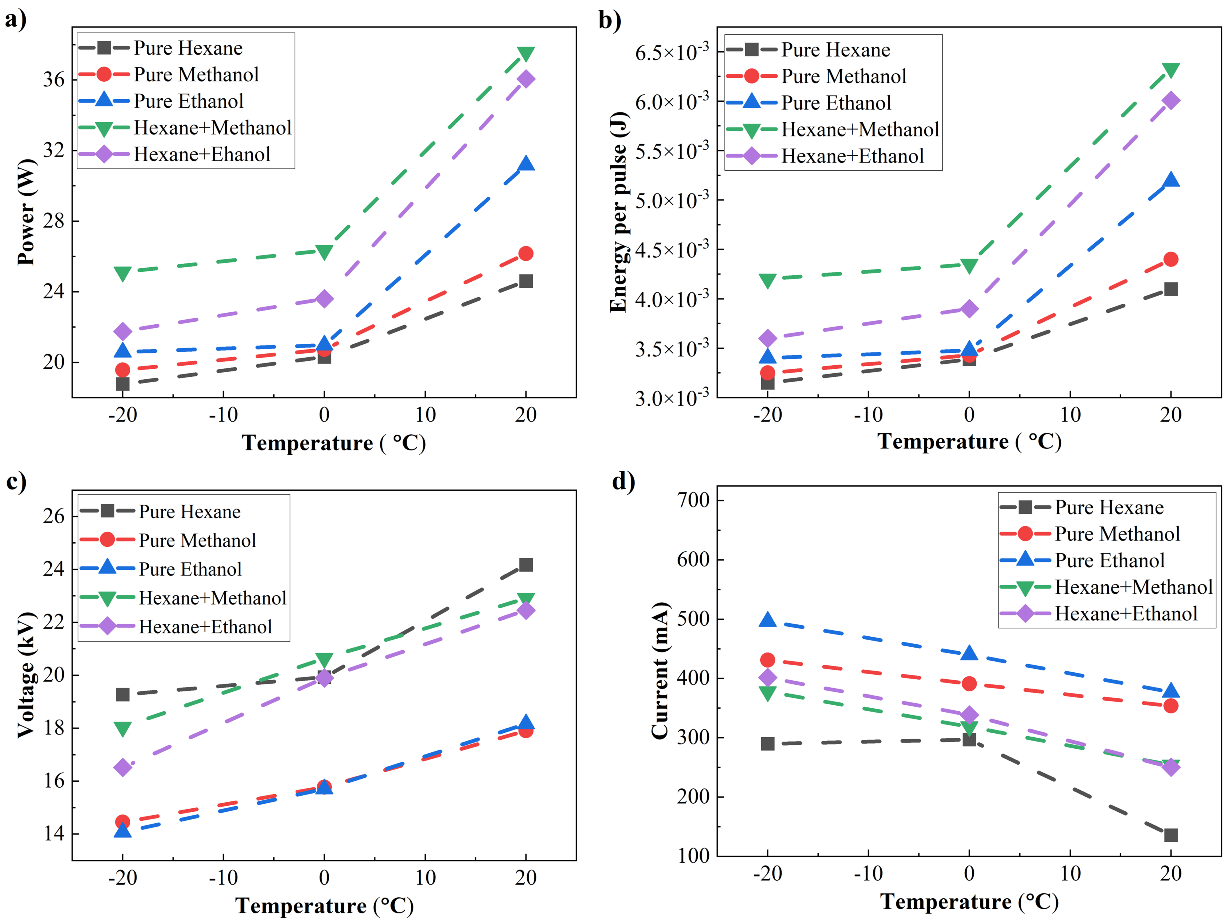

Figure 3.13: Variation of (a) Power (W), (b) Energy per pulse (J), (c) voltage (kV), and (c) current (mA) with temperature of different mixture reforming

Previously reported studies observed changes in dissipated power with vapor content that were closely monitored in our study [118]. The dielectric permittivity (ϵ) of the liquid plays a crucial role in breakdown voltages and the vapor pressure determines its vapor content in the gas phase [8]. In our selected liquids hexane has the highest Pv at 20 °C and the lowest ϵ of 1.87 [119], which accounts for the high voltage, 24.17 kV, and low current, 135.73 mA, as seen from Figure 3.13c and Figure 3.13d. It is thus evident that the gas gap was harder to break down, and it was difficult to have a high flow of electrons in the system. The high content of hexane vapor can further quench down the excited particles inhibiting the ionization of the argon gas. Hexane-methanol mixture which has the next highest vapor pressure, due to the presence of methanol with an ϵ of $\approx$ 33.10 [120], shows a lower breakdown voltage of 22.9 kV and higher current of 254.33 mA. Similarly, the other treatment mixtures follow the expected results, with alcohols giving the lowest breakdown voltages and highest currents, that depend on their vapor pressure and dielectric permittivity as can be seen from Figures 3.13 c and 3.13 d. Also, as we decreased the reactor temperature from 20 °C to -20 °C we observed a significant decrease in the power and energy for all the liquids which attributes to the lower hydrocarbon vapor content with mostly argon dominating in the gas phase. Hexane-alcohol mixtures supplied higher power and energy to the system followed by the alcohols, whereas hexane provided the least power and energy as can be seen from Figure 3.13a and Figure 3.13b.

3.6.3 Gas sample characterization

The gas sample was collected into Tedlar® gas sampling bags (1 L volume) from Chromatographic Specialities Inc and was analyzed using a GC-TCD (gas chromatography – thermal conductivity detector). 1 ml of the gas was injected into the GC-TCD for characterization. Table 3.2. shows the detailed method used in the TCD. A gas standard containing mixture of various hydrocarbon and inorganic gases was bought from MESA gas for making the calibration curve. Figure 3.14. represents the chromatogram of the gas standard. The calibration curve was made using 1 ml, 0.50 ml, and 0.20 ml injection volume. Table 3.4. contains the details of each peak along with the calibration slopes with R^2 values. It should be noted that the intercept of the calibration curve was set to 0 as we observed a flat line with no peaks of HCs for air injection. Y=mX form was used for the calibration of the gas standard where Y is the volume injected, X is the peak area and m is the slope.

Table 3.2: GC-TCD method for gas analysis

Parameters	**Set Conditions**
Column	1. HP Plot-Q: 30m x 0.530mm, 40.00 micron
	2. HP-PLOT MoleSieve: 30m x 0.530mm, 50.00 micron
Carrier	Argon @ 7 ml/min
Switching conditions	0-5 min → both columns open
	5 min → column 2 closed
	28 min → both columns open
Oven	30 °C hold 5.50 min
	10 °C/min to 175 °C hold 8.10 min
	25 °C/min to 150 °C hold 5.90 min

Injector	Split/splitless; split flow: 5:1 Temperature: 200 °C
Detector	TCD, 250 °C

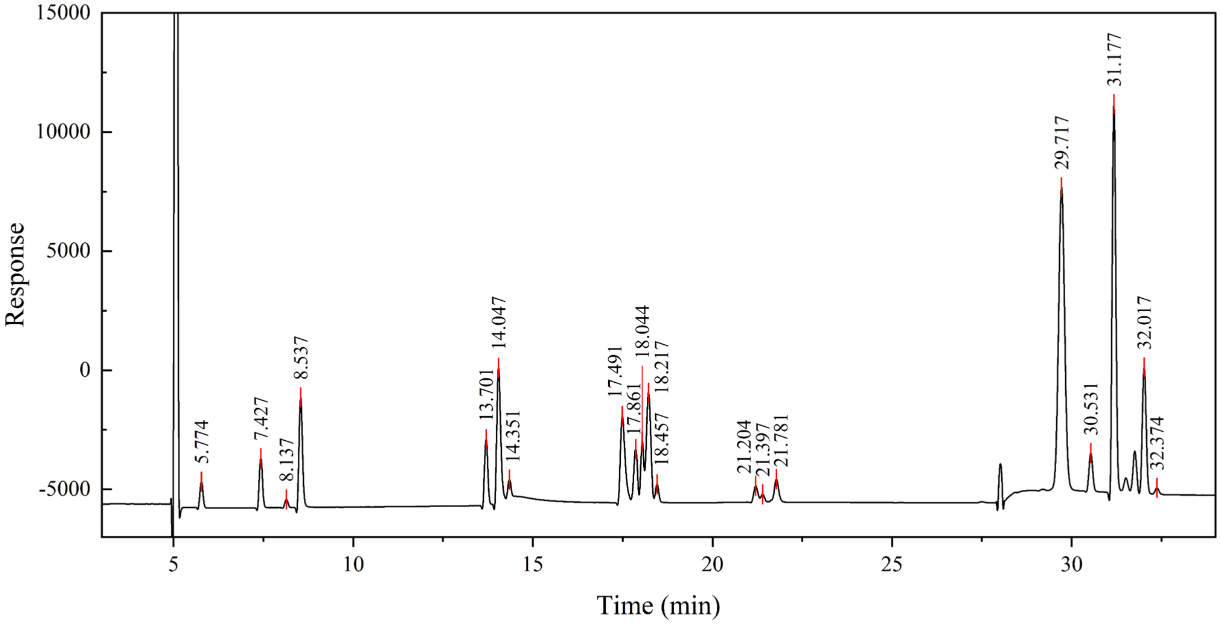

Figure 3.14: Chromatogram of gas standard as observed in the GC-TCD

Table 3.4: The retention time of different gases in the standard gas mixture along with the calibration coefficients

Retention Time (min)	Compound	Slope	R^2
5.774	CO_2	73.924	0.99
7.427	Ethylene	138.55	0.98

8.137	Acetylene	49.039	0.99
8.537	Ethane	333.65	0.98
13.701	Propylene	202.02	0.99
14.047	Propane	474.38	0.99
14.351	Propadiene	52.112	0.99
17.491	Isobutane	388.76	0.99
17.861	Trans-2-butene	202.41	0.99
18.044	N-butane	194.38	0.99
18.217	1,3 butadiene	493.39	0.99
18.457	Cis-2-butene	64.631	0.99
21.204	Isopentane	68.844	0.99
21.397	1-pentene	30.005	0.99
21.781	N-pentane	86.037	0.98
29.717	H_2	1784.9	0.99
30.531	O_2	65.606	0.99
31.177	N_2	1069.9	0.99
32.017	CH_4	411.62	0.99
32.374	CO	21.74	0.99

The data for gas samples are presented as groups of carbon families of C1, C2, C3, and so on. In each data set, the gases were individually identified by comparing them with our standard mixture. All the individually calculated gas productions were then grouped in the paper according to their carbon number to provide an overall overview of the plasma-chemical reactions. Figure 3.15. shows the different gases produced from each experiment at 20 ℃.

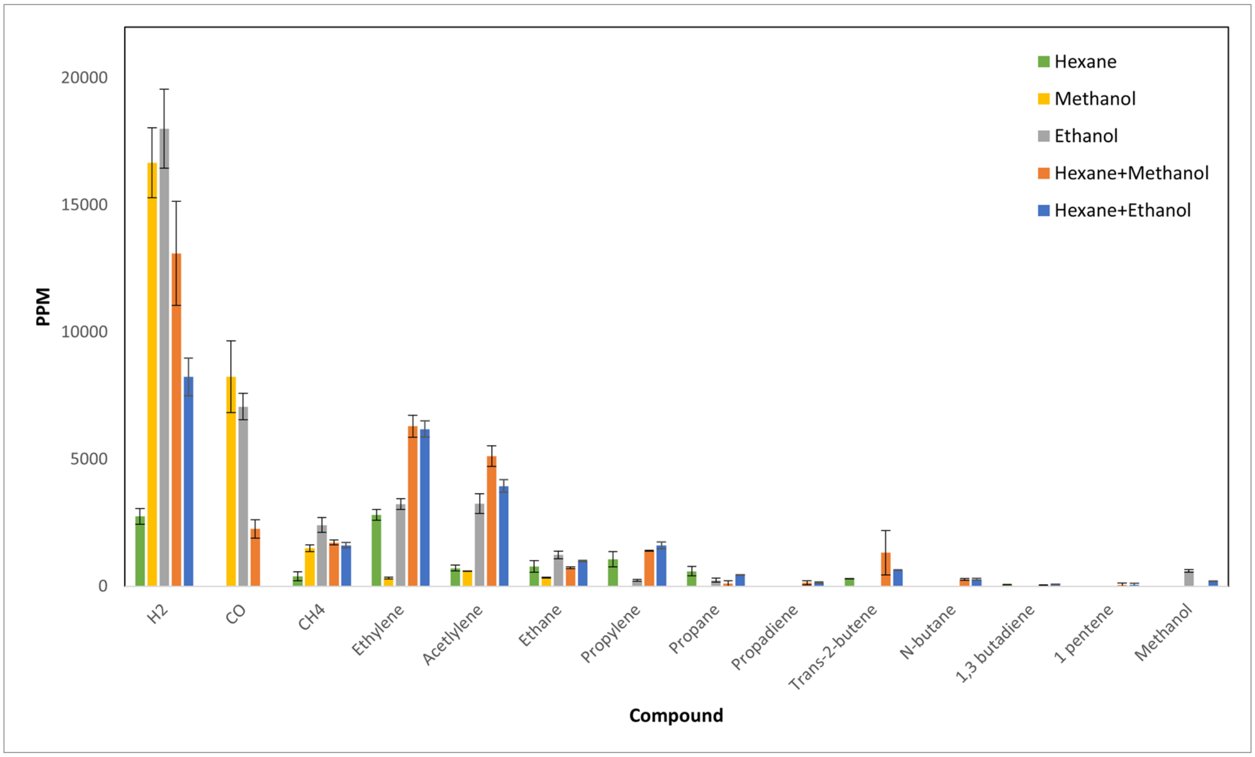

Figure 3.15: Different gas compounds formed in ppm (mol) from plasma treatment at 20 ℃ of different liquids

3.6.4 Effect on the production of hydrogen and/or syngas

The effect of plasma treatment of different hydrocarbon mixtures as well as the temperature variation was closely monitored to understand its influence on syngas production. In hexane and hexane-alcohol mixtures, CO was either not produced or was produced in insignificant amounts as opposed to pure methanol/ethanol. Figure 3.16. shows the selectivity and H_2/CO ratio in methanol and ethanol. In methanol, the selectivity of both H_2 and CO was higher than in ethanol at all the tested temperatures. The H_2/CO ratio was between 2 and 2.8 in methanol and ethanol. The reactions associated with the decomposition of methanol and ethanol to syngas can be the following [121, 122]:

$$\mathrm{CH_3OH} \longrightarrow 3\,\mathrm{H_2} + \mathrm{CO} \tag{3.5}$$

$$\mathrm{C_2H_5OH} \longrightarrow 2.5\,\mathrm{H_2} + \mathrm{CO} + 0.5\,\mathrm{C_2H_2} \tag{3.6}$$

Our syngas production ratio was very close to the associated chemical reactions which are 2.5 and 3. The slight differences could be due to the large number of by-products formed during the decomposition process. The H_2/CO ratio did not change much with temperature and stayed within the expected range and thus it can be concluded that reactor temperature has very less influence on the selectivity of syngas production. A flexible H_2/CO ratio is important for decreasing capital investment and operating cost and a stoichiometric ratio of ≈ 2 is optimum to meet industrial standards [123]. In a previously reported study, it was also found that a high H_2/CO ratio, anything greater than 1, on fuel combustion is favorable to decreasing the HC emissions which is also true for our study [124].

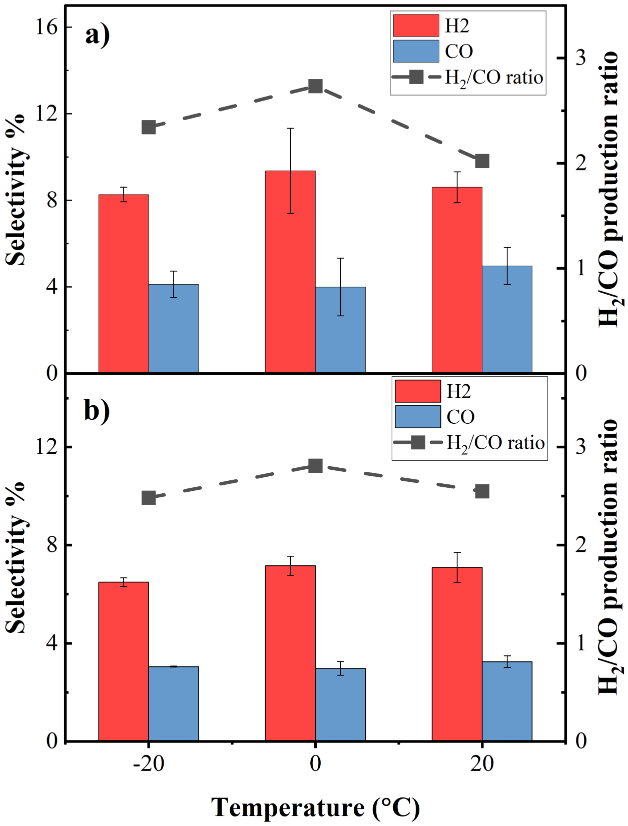

Figure 3.16: Variation of Selectivity % and H_2/CO production ratio for (a) methanol and (b) ethanol at different temperatures

3.6.5 Liquid sample characterization

The liquid samples were collected into GC amber vials and 1 µl was injected into the GC-MS (gas chromatography-mass spectrometry) for its characterization. Table 3.6. shows the detailed method used in the MS. A liquid standard of 1000 ppm of C7-C30 each in hexane was bought from Sigma-Aldrich for calibration. Figure 3.17. represents the chromatogram of the standard mixture. The standard was diluted 10, 100, and 1000 times and was simultaneously weighted for accuracy to obtain 132 ppm, 13 ppm and 1.34 ppm respectively. The calibration curve was then made using the prepared standard. Table 3.7. contains the details of each peak along with the calibration slopes with R2 values. It should be noted that the intercept of the calibration curve was set to 0 as we observed a flat line with no peaks of HCs for a blank injection of solvent. Y=mX form was used for the calibration of the gas standard where Y is the ppm injected, X is the peak area and m is the slope.

Table 3.6: GC-MS method for analysis of liquid samples

Parameters	**Set Conditions**
Column	Rxi - 5 ms: 30m x 0.25mm, 25.00 micron
Carrier	Helium @ 1.2 ml/min
Oven	40 °C hold 2 min
	15 °C/min to 300 hold 5 min
Injector	Split/splitless; split flow: 20:1
	Temperature: 250 °C

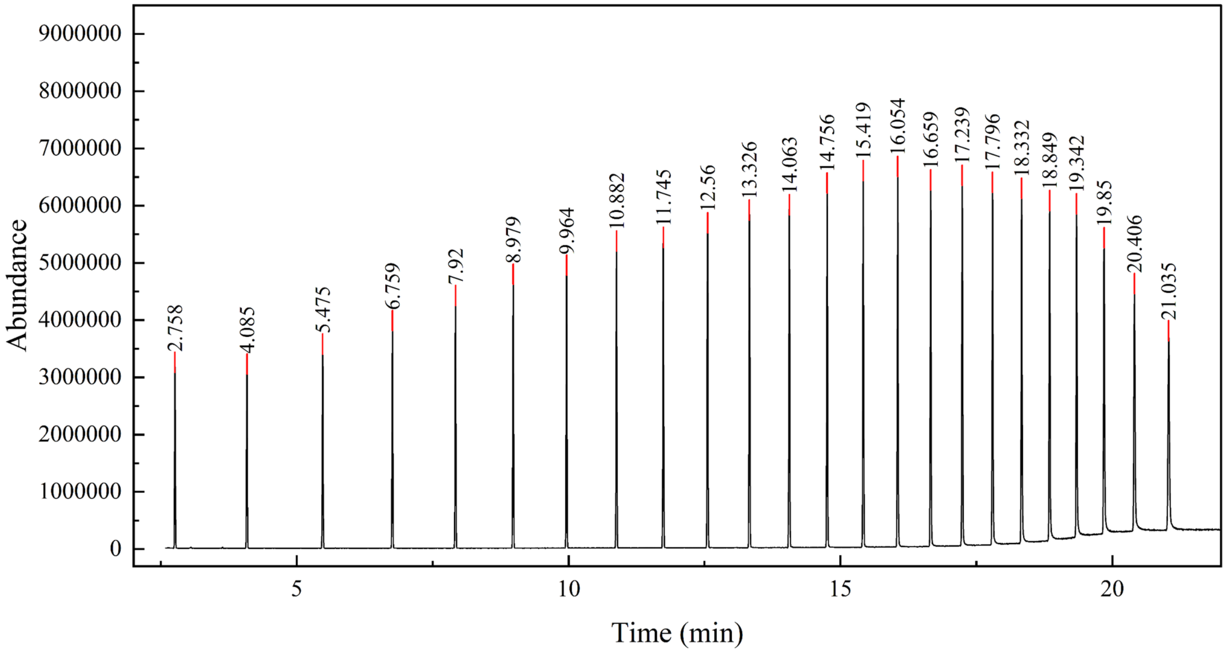

Figure 3.17: Chromatogram of liquid standard as observed in the GC-MS

Table 3.7: Liquid standard along with their calibration constants

Alkane	**Retention Time (min)**	**Slope**	**R^2**
C7	2.762	243256	0.99
C8	4.085	258897	0.99
C9	5.479	283082	0.99
C10	6.761	314069	0.99
C11	7.921	348905	0.99
C12	8.981	347329	0.99
C13	9.964	402666	0.99

C14	10.882	428644	0.99
C15	11.745	455422	0.99
C16	12.559	483579	0.99
C17	13.33	500442	0.99
C18	14.062	517001	0.99
C19	14.759	530642	0.99
C20	15.422	549880	0.99
C21	16.056	563908	0.99
C22	16.662	565443	0.99
C23	17.243	576491	0.99
C24	17.799	580007	0.99
C25	18.334	580729	0.99
C26	18.849	556721	0.99
C27	19.345	570163	0.99
C28	19.851	535948	0.99
C29	20.409	541850	0.99
C30	21.039	522728	0.99

The liquid products formed were identified using the NIST08.l library of the MS and was accordingly grouped into C7, C8, C9, C10 and so on of carbon families. It was assumed that everything lower than hexane were mostly formed in the gas phase of our experiments and was identified using the TCD. A large solvent blow into the MS detector is not desirable and so it had a solvent delay of 2.5 mins, and it was only possible to detect compounds that comes after the solvent peak. The calibration coefficients used for different products were based on where the peaks lie, for example, if the peak lied at 3.5 min the calibration coefficient of C8 was used. Figure 3.18. shows the MS spectra of hexane and its mixture with alcohols at 20 ℃ which indicates the formation of many compounds due to plasma-chemical reactions. It should be noted that the products formed for each treated liquid remained the same across different set of experiments however their concentrations varied across different operating conditions.

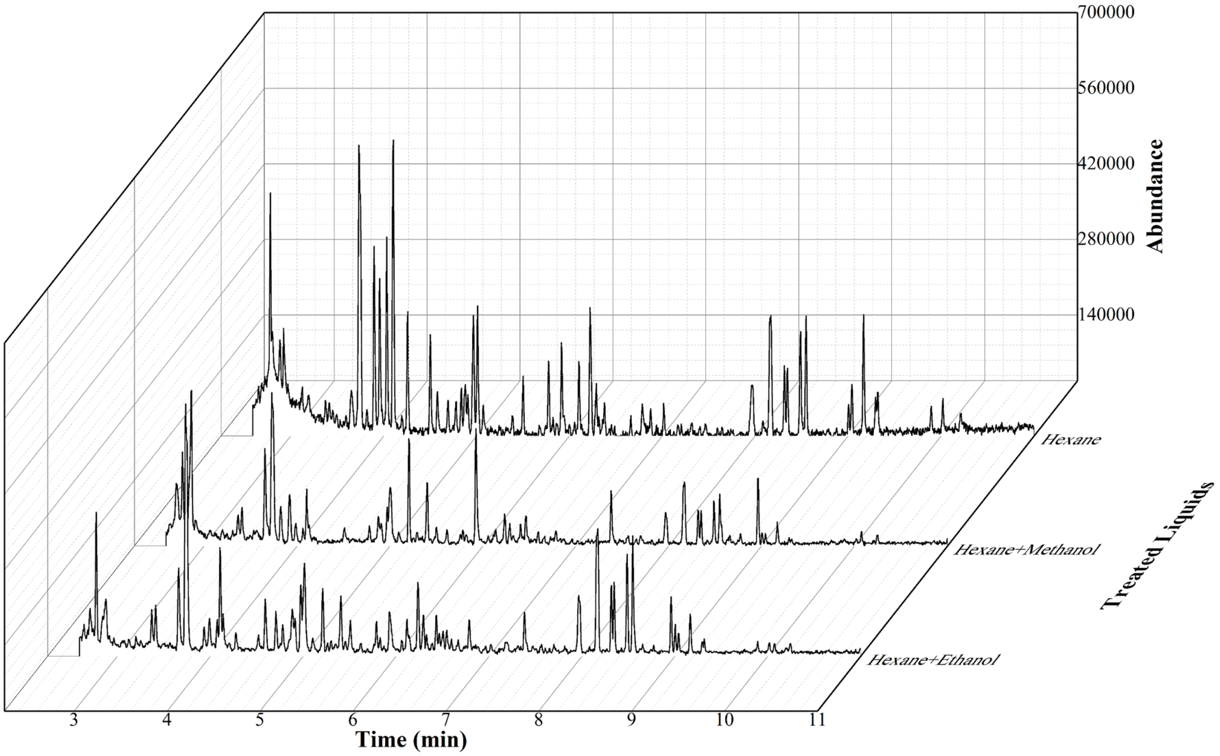

Figure 3.18: GC-MS spectra of different liquid treatments at 20 ℃

Pure alcohol treatments were not considered as they provided only oxygenated compounds which was not the focus of these experiments. Figure 3.19. shows the GC-MS spectra of methanol and ethanol at 20 ℃. The single peak of methanol treatment was identified to be ethylene glycol which is an interesting find for future experiments that could be focused on glycol productions from simple alcohols. Ethanol treatment produced a greater range of compounds which were mainly butanol, pentanol, hexanol and their isomers. Pure alcohols also showed similar trend of higher production efficiency at lower temperatures as reported in the paper for hexane-alcohol mixtures.

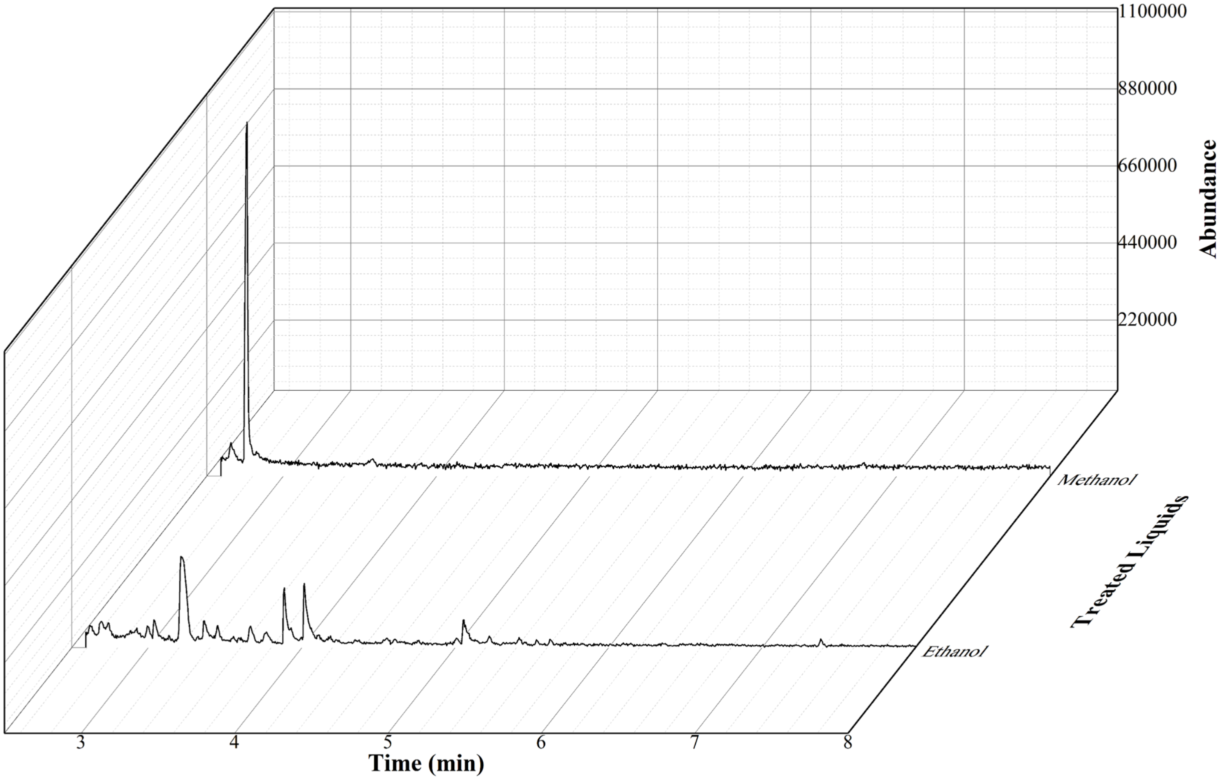

Figure 3.19: GC-MS spectra of pure methanol and pure ethanol treatments at 20 ℃

Table 3.9. lists all the compounds as identified by the GC-MS from different treated liquids. Figure 3.20 provides an overview of the concentration of products formed at different treatments from which further calculations were made in the paper.

Table 3.9: List of compounds identified for plasma treatment of different liquids with the GC-MS

Compound	**Structure**
heptane	
butane 2-ethoxy 2-methyl	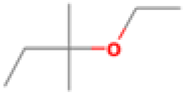
1-pentene 3-ethyl 2-methyl	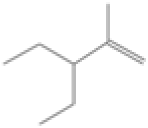
1-butanol 3-methyl	
toluene	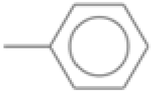
hexane 3-ethyl	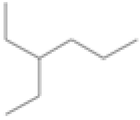
3-hexanone	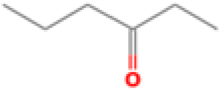
2-hexanone	

3-hexanol	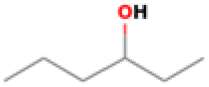
octane	
2-heptanol 3-methyl	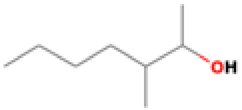
3-heptanol	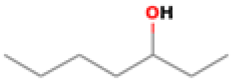
2-butanol 3-methyl	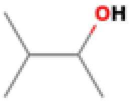
octane 4,5 diethyl	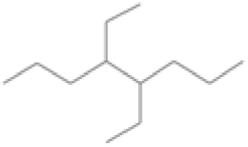
heptane 2,3 dimethyl	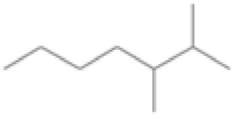
heptane 4-ethyl	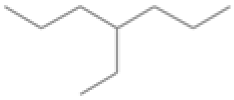
octane 4-methyl	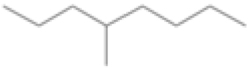
1-hexanol	

phenylethyne

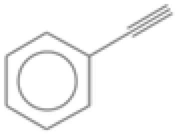

styrene

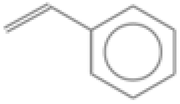

heptane 1-ethoxy

nonane

hexane 3-ethyl 2-methyl

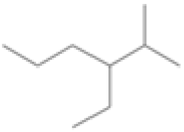

octane 3,4 dimethyl

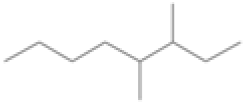

hydroperoxide 1-ethyl

butyl

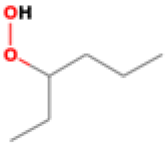

1-pentanol 2,2 dimethyl

nonane 5-methyl

decane 5,6 dimethyl	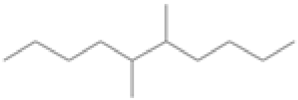
2-heptanol 3-methyl	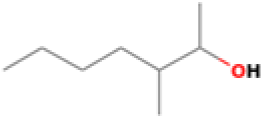
octane 4,5 diethyl	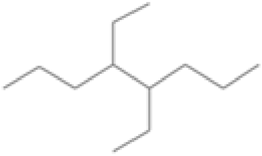
decane 5,6 dimethyl	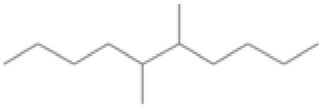
undecane 4,4 dimethyl	
undecane 5-methyl	
naphthalene	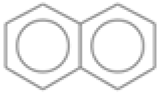
dodecane	

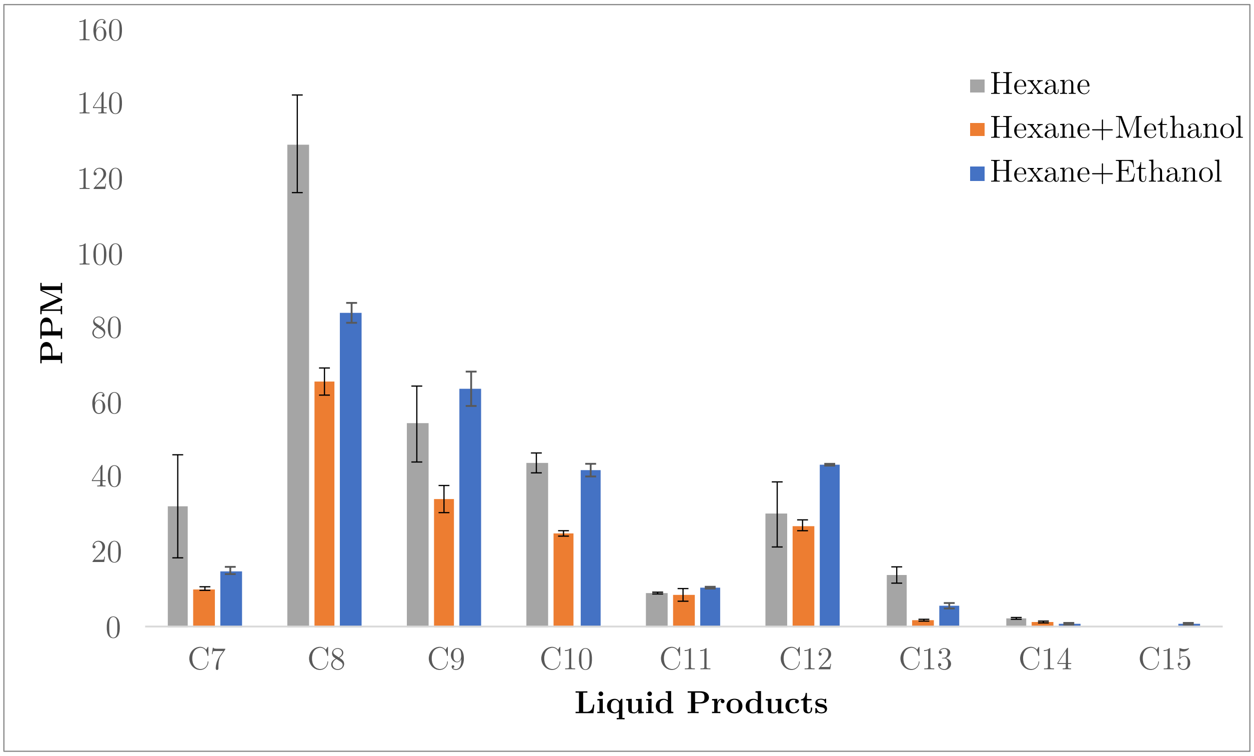

Figure 3.20: Concentration of liquid products from different treated liquids at 20 ℃

3.6.6 Effect of temperature on liquid selectivity

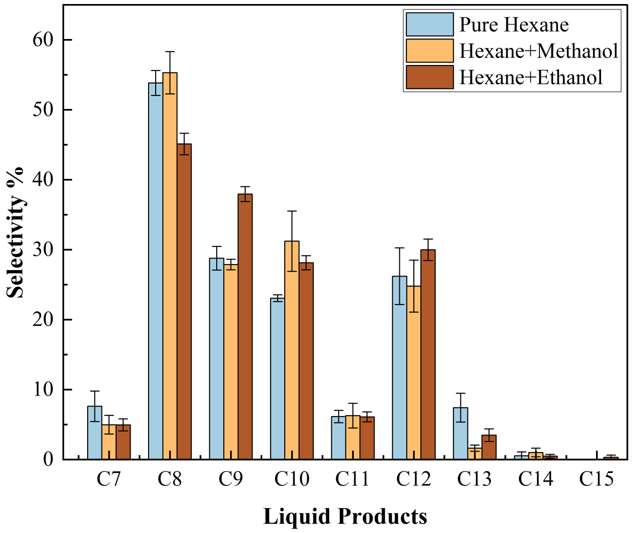

Figure 3.21: Average of liquid product selectivity % across different temperatures for treatment of pure hexane, hexane+methanol, and hexane+ethanol.

An average of selectivity at different temperatures is shown in Figure 3.21. for each treated liquid. The selectivity of C8, C9, C10, and C12 were found to be higher with hexane-alcohol mixtures giving higher selectivities. Hexane-methanol showed selectivities of 55.3%, 31.2% for C8 and C10 while hexane-ethanol showed selectivities of 37.9%, 30% for C9 and C12 products.

3.6.7 Chemical Assessment of Products

The number of moles, n_i, produced of each gas product can be given as

$$n_i = \dot{n}_i \times t \tag{3.7}$$

Where $\dot{n}_i$ is the molar flowrate from the exit stream of the reactor and t is the plasma treatment time which was fixed at 20 min for all the experiments. Production efficiency of gas products, $\eta_g(mmol/kWh)$, can then be calculated as

$$\eta_g = \frac{n_i \times 1000}{E_{pulse} \times t \times 2.77 \times 10^{-7}} \tag{3.8}$$

Where n_i is in moles, E_{pulse} is in J. The relative yield, RE, of each gas product is calculated as follows when N_{gas} is the total number of gas products formed.

$$RE\% = \frac{n_i}{\sum_{i=1}^{N_{gas}} n_i} \times 100 \tag{3.9}$$

The selectivity of the produced H_2 ($S_{(H_2)}$) is given by

$$S_{(H_2)}\% = \frac{1}{7} \frac{n_{(H_2)}}{\sum_{(i=1)}^{N_{gas}} n_i} \times 100 \tag{3.10}$$

The selectivity of the gas products having x carbon atoms (S_i) is given as follows

$$S_i\% = \frac{x}{6}\frac{n_i}{\sum_{(i=1)}^{N_{gas}} n_i} \times 100 \tag{3.11}$$

To assess the liquid products, a similar method was used. The production efficiency, η_l (g/kWh), and selectivity (S_j) of products having y carbon atoms was calculated with the following equations.

$$\eta_l = \frac{C_j \times V_{liq}}{E_{pulse} \times t \times 2.77 \times 10^{-7}} \tag{3.12}$$

$$S_j\% = \frac{y}{6}\frac{C_j}{\sum_{j=1}^{N_{liq}} C_j} \times 100 \tag{3.13}$$

Where V_{liq} is the volume of the liquid used for treatment, C_j is the concentration of j^{th} liquid product in mg/L and N_{liq} is the total number of liquid products formed.

Chapter 4

Summary & Outlook

4.1 Discussion

This thesis encompasses the use of non-thermal plasma for the chemical synthesis of organic compounds. An NTP reactor was designed and constructed to carry out chemical transformations. The main products obtained in the gas phase comprised of H_2, CO, and C1-C4 HCs (methane, ethane, ethylene, acetylene, propylene, propadiene, butane, isobutane, butadiene). The liquid products consisted of higher HCs (C7-C15), and the treatment of hexane-alcohol mixture contained a mix of HCs and oxygenates.

The type of discharge can also play a crucial role in the system efficiency. Pulsed discharges are known to produce higher electric fields than other kinds of continuous discharges. Among pulsed discharges, microsecond discharge has the advantage of both millisecond and nanosecond discharge, as it is not too weak for electron excitation or too strong for electrical interference between equipment. Thus for our experiments, a microsecond pulsed DBD reactor was designed and constructed.

In this thesis, the role of non-thermal plasma in fuel reforming has been investigated. Conventional methods of fuel reforming, like steam reforming, are very energy-intensive as they operate under high temperature and/or high pressure. Further, these processes are subject to catalyst requirement, which needs to be reactivated later. Whereas, NTP is a clean process that can aid in fuel reforming. The non-equilibrium nature can enable thermodynamically unfavorable reactions to proceed at low temperatures. They do not require any catalyst for their operation and are portable with the ability for in-situ operation. Recent investigations of gas temperature on hydrocarbons have further opened up new paths of exploration for reforming processes using NTP.

In the experiments, NTP was investigated as a technology to synthesize H_2, crack HCs, and produce more complex valuable chemicals. The effect of reactor temperature and the addition of alcohols to n-hexane was studied. The temperature affected the production efficiency, but the products obtained at different temperatures remained the same. It can be said that the temperature/characteristics of the plasma do not change much with the reactor temperature as discussed in Chapter 2. The production efficiency was found to increase for liquid products at a lower temperature. The selectivity of liquid products showed no major change with temperature.

The effect of the addition of alcohols was also studied. Higher hydrocarbons in the gas phase increased with liquid products, and with ethanol treatment negligible amounts of methanol was observed. The amount of syngas produced also increased with the addition of alcohols. However, with the addition of alcohols, the production efficiency of the liquid products decreased, which could be associated with the alcohols' quenching effect.

Overall, NTP was proven to be successful for fuel transformation. Its ability to perform multiple operations at once, like H_2 production, cracking of heavy oils, and synthesizing higher complex compounds in the liquid phase, makes it an attractive technology for both the fuel and chemical industry. Its ambient operating conditions and low energy requirements further make it an interesting field of research.

4.2 Conclusion

The following conclusions were made from this project with regard to the objective of this thesis.

1. **Design and construction of a pin-to-plate microsecond pulsed plasma reactor -** The reactor was successfully constructed and was able to give results relevant to our objectives.

2. **Optimization of operating parameters -** The reactor temperature was controlled to reduce the effect of vapor pressure in the discharge region. It was observed that

the breakdown voltage decreased at lower temperatures. The liquid products formed increased at lower temperatures, and for the gas products it decreased, owing to the low amounts of vapor in the gas phase.

3. **Use of n-hexane as a model hydrocarbon -** It has the highest vapor pressure among all the compounds and produced a range of HCs (C1-C5) in the gas phase along with H_2 and higher HCs in the liquid phase.

4. **Addition of methanol and ethanol -** The addition of ethanol produced more products both in the gas phase and the liquid phase, which could be associated with the extra C present in ethanol. However, in the liquid products, the addition of alcohols decreased the production efficiency, which could be due to the quenching effect of alcohols.

5. **Plasma chemistry of organic synthesis -** An insight into the plasma chemistry was gained from the products. Reactions mostly seemed to undergo dehydrogenation and dissociation.

4.3 Future Work

The work carried out can be expanded to increase the efficiency and scalability of such processes. Some recommendations for future work are listed below.

1. **Use of multi-pin discharge and/or multiple reactors in series.** This could increase the contact area of the plasma, leading to more product formation.

2. **Use of optical emission spectrometer (OES) and laser technology to capture the radicals formed during reactions.** This could shed more light on the plasma chemistry of the system.

3. **Use of gas recycling methods.** The gas from the exit stream could be recycled into the reactor to alter the selectivity of certain products.

4. **Addition of catalysts.** This could be an important area of investigation as certain plasma-catalytic reactors have shown to selectively form certain products with good efficiency, and it could be interesting to test it out in the context of our reactor.

Appendix

Standard operating procedure for plasma-treatment of liquids

1. Open the fume hood.
2. Start the water-cooling system. Set the desired temperature and the pump to 90. If bubbles remain in the jackets, turn the reactor to let the bubbles escape by the exiting stream.
3. Pour the required volume of desired liquid into the reactor.
4. Start the gas flow of air by opening the tank valve and setting the pressure regulator to 10 psi. Adjust the flowmeter to have the desired value. Check for gas leakage with the “snoop” soapy solution.
5. Turn the drain valve at the bottom of the reactor gradually to let gas flow inside. Turn it until the gas continues sparging without interruption.
6. Place the stainless-steel wire at the negative side of the transformer in the current

monitor and attach the stainless-steel wire to the bottom electrode. Put bubble wrap in the hole of the current monitor to ensure that the stainless-steel wire is in the middle of the hole.

7. Connect the ground wire to the stainless-steel wire immediately after the negative outlet of the transformer.

8. Close the reactor lid with the green quick-release stainless-steel camp.

9. Place the top electrode at the predetermined height for the experiment. Make sure not to have any water droplets on the top electrode. If it is the case, remove the top electrode, wash it with brown paper, and put it back in place.

10. Connect the transformer to the top electrode by placing the ring of the transformer's wire on the top electrode. To ensure proper electrical contact throughout the experiment, place a crocodile clip connecting the two pieces of equipment.

11. Connect the voltage probe to the top electrode by placing a crocodile clip connecting the two pieces of equipment. Stabilize the voltage probe with a three-finger clamp connected to the laboratory stand support.

12. Close the fume hood completely and turn on the pulse generator supply.

13. Decrease the voltage to 0 V and turn on the power supply. Set the frequency to 6 kHz for organic liquids (Tested frequencies through a few experiments for a stable

discharge). Then, gradually increase the voltage to 300 V for organic liquids on the power supply, which will generate a voltage of around 10 kV between the pin and the water. The presence of plasma can be confirmed visually with the naked eye by a bright blue-ish color.

14. Let the system operate while monitoring the electrical signals, flow rates, and plasma stability for the desired plasma treatment time.

15. Collect the gas sample into the Tedlar bag just before ending the plasma treatment, to be later analyzed using GC-TCD.

16. At the end of plasma treatment, turn down the voltage to 0V and close the power generator.

17. Open the fume hood and ground all metal pieces with the ground wire to avoid any incidental electrical discharge.

18. Collect the liquid sample into GC vials and characterize it using GC-MS later.

19. At the end of the day, close the flowmeter, close the air inlet, close the water-cooling system, drain the gas line, and dispose of any remaining plasma-treated water in a special waste container or store it in glass vials for further analysis.

Bibliography

[1] J. Artz, T. E. Muller, K. Thenert, J. Kleinekorte, R. Meys, A. Sternberg, A. Bardow, and W. Leitner, "Sustainable conversion of carbon dioxide: an integrated review of catalysis and life cycle assessment," *Chemical reviews*, vol. 118, no. 2, pp. 434–504, 2018.

[2] M. Muntean, D. Guizzardi, E. Schaaf, M. Crippa, E. Solazzo, J. Olivier, and E. Vignati, "Fossil co2 emissions of all world countries," *Luxembourg: Publications Office of the European Union*, vol. 2, 2018.

[3] K. Wang, H. R. Damarla, I. C. Berman, and D. Staack, "High dose rate electron beam irradiation of heavy alkanes in a multi-phase flow system," *Fuel*, vol. 274, p. 117695, 2020.

[4] M. Alfi, M. A. Barrufet, R. G. Moreira, P. F. Da Silva, and O. C. Mullins, "An efficient treatment of ultra-heavy asphaltic crude oil using electron beam technology," *Fuel*, vol. 154, pp. 152–160, 2015.

[5] S. Y. A. Siddiki, M. Mofijur, P. S. Kumar, S. F. Ahmed, A. Inayat, F. Kusumo, I. A. Badruddin, T. Y. Khan, L. Nghiem, H. C. Ong, *et al.*, "Microalgae biomass as a sustainable source for biofuel, biochemical and biobased value-added products: An integrated biorefinery concept," *Fuel*, vol. 307, p. 121782, 2022.

[6] A. V. Tavasoli, M. Preston, and G. Ozin, “Photocatalytic dry reforming: what is it good for?,” *Energy & Environmental Science*, vol. 14, no. 5, pp. 3098–3109, 2021.

[7] K. Wang, S. I. Bhuiyan, M. A. H. Baky, J. Kraus, C. Campbell, H. Jemison, and D. Staack, “Electric fuel conversion with hydrogen production by multiphase plasma at ambient pressure,” *Chemical Engineering Journal*, vol. 433, p. 133660, 2022.

[8] A. Hamdan, J.-L. Liu, and M. S. Cha, “Transformation of n-heptane using an in-liquid submerged microwave plasma jet of argon,” *Journal of Applied Physics*, vol. 129, no. 4, p. 043303, 2021.

[9] P. Bruggeman and C. Leys, “Non-thermal plasmas in and in contact with liquids,” *Journal of Physics D: Applied Physics*, vol. 42, no. 5, p. 053001, 2009.

[10] A. Bogaerts and E. C. Neyts, “Plasma technology: an emerging technology for energy storage,” *ACS Energy Letters*, vol. 3, no. 4, pp. 1013–1027, 2018.

[11] P. Bruggeman, A. Bogaerts, J. Pouvesle, E. Robert, and E. Szili, “Plasma–liquid interactions,” 2021.

[12] P. Bruggeman, M. J. Kushner, B. R. Locke, J. G. Gardeniers, W. Graham, D. B. Graves, R. Hofman-Caris, D. Maric, J. P. Reid, E. Ceriani, *et al.*, “Plasma–liquid interactions: a review and roadmap,” *Plasma sources science and technology*, vol. 25, no. 5, p. 053002, 2016.

[13] A. Sun, C. Huo, and J. Zhuang, “High voltage 1 (2), 74–80 (2016),” 2016.

[14] B. R. Locke and S. M. Thagard, “Analysis and review of chemical reactions and transport processes in pulsed electrical discharge plasma formed directly in liquid water,” *Plasma Chemistry and Plasma Processing*, vol. 32, no. 5, pp. 875–917, 2012.

[15] J. Kolb, R. Joshi, S. Xiao, and K. Schoenbach, “Streamers in water and other dielectric liquids,” *Journal of Physics D: Applied Physics*, vol. 41, no. 23, p. 234007, 2008.

[16] S. Gershman, O. Mozgina, A. Belkind, K. Becker, and E. Kunhardt, “Pulsed electrical discharge in bubbled water,” *Contributions to Plasma Physics*, vol. 47, no. 1-2, pp. 19–25, 2007.

[17] H. Wang, R. J. Wandell, K. Tachibana, J. Voráč, and B. R. Locke, “The influence of liquid conductivity on electrical breakdown and hydrogen peroxide production in a nanosecond pulsed plasma discharge generated in a water-film plasma reactor,” *Journal of Physics D: Applied Physics*, vol. 52, no. 7, p. 075201, 2018.

[18] S. Wang, Y. Liu, R. Zhou, F. Liu, Z. Fang, K. K. Ostrikov, and P. J. Cullen, “Microsecond pulse gas–liquid discharges in atmospheric nitrogen and oxygen: Discharge mode, stability, and plasma characteristics,” *Plasma Processes and Polymers*, vol. 18, no. 2, p. 2000135, 2021.

[19] H. Zeghioud, P. Nguyen-Tri, L. Khezami, A. Amrane, and A. A. Assadi, “Review on discharge plasma for water treatment: mechanism, reactor geometries, active species and combined processes,” *Journal of Water Process Engineering*, vol. 38, p. 101664, 2020.

[20] N. Shirai, S. Uchida, and F. Tochikubo, “Influence of oxygen gas on characteristics of self-organized luminous pattern formation observed in an atmospheric dc glow discharge using a liquid electrode,” *Plasma Sources Science and Technology*, vol. 23, no. 5, p. 054010, 2014.

[21] V. Scholtz, J. Pazlarova, H. Souskova, J. Khun, and J. Julak, “Nonthermal plasma—a tool for decontamination and disinfection,” *Biotechnology advances*, vol. 33, no. 6, pp. 1108–1119, 2015.

[22] P. Bruggeman, J. Liu, J. Degroote, M. G. Kong, J. Vierendeels, and C. Leys, "Dc excited glow discharges in atmospheric pressure air in pin-to-water electrode systems," *Journal of Physics D: Applied Physics*, vol. 41, no. 21, p. 215201, 2008.

[23] S. Zhang and T. Dufour, "Self-organized patterns by a dc pin liquid anode discharge in ambient air: Effect of liquid types on formation," *Physics of Plasmas*, vol. 25, no. 7, p. 073502, 2018.

[24] G. Neretti, M. Taglioli, G. Colonna, and C. Borghi, "Characterization of a dielectric barrier discharge in contact with liquid and producing a plasma activated water," *Plasma Sources Science and Technology*, vol. 26, no. 1, p. 015013, 2016.

[25] W. Harrison, W. Hang, X. Yan, K. Ingeneri, and C. Schilling, "Temporal considerations with a microsecond pulsed glow discharge," *Journal of Analytical Atomic Spectrometry*, vol. 12, no. 9, pp. 891–896, 1997.

[26] V. I. Gibalov and G. J. Pietsch, "Dynamics of dielectric barrier discharges in different arrangements," *Plasma Sources Science and Technology*, vol. 21, no. 2, p. 024010, 2012.

[27] Z. Zhao, J.-M. Li, J. Zheng, Y. Cui, and B. C. Khoo, "Study of shock and induced flow dynamics by nanosecond dielectric-barrier-discharge plasma actuators," *AIAA Journal*, vol. 53, no. 5, pp. 1336–1348, 2015.

[28] L. Xie, H. Liang, J. Li, *et al.*, "Experimental investigation of hysteresis effect by microsecond pulse plasma actua-tor," *Journal of Propulsion Technology*, vol. 40, no. 10, pp. 2216–2225, 2019.

[29] T. Zhao, Q. Zhang, B. Zheng, Y. Liu, Y. Jin, and Q. Chen, "Electrical and aerodynamic characteristics of sliding discharge based on a microsecond pulsed plasma supply," *Plasma Science and Technology*, 2022.

[30] P. Bruggeman, J. L. Walsh, D. C. Schram, C. Leys, and M. G. Kong, “Time dependent optical emission spectroscopy of sub-microsecond pulsed plasmas in air with water cathode,” *Plasma Sources Science and Technology*, vol. 18, no. 4, p. 045023, 2009.

[31] N. Bolouki, W.-H. Kuan, Y.-Y. Huang, and J.-H. Hsieh, “Characterizations of a plasma-water system generated by repetitive microsecond pulsed discharge with air, nitrogen, oxygen, and argon gases species,” *Applied Sciences*, vol. 11, no. 13, p. 6158, 2021.

[32] F. Song, Y. Wu, S. Xu, D. Jin, and M. Jia, “N-decane decomposition by microsecond pulsed dbd plasma in a flow reactor,” *International Journal of Hydrogen Energy*, vol. 44, no. 7, pp. 3569–3579, 2019.

[33] Z. Fan, H. Sun, S. Zhang, W. Han, C. Zhang, Q. Yang, and T. Shao, “Cox-free co-cracking of n-decane and ch4 to hydrogen and acetylene using pulsed spark plasma,” *Chemical Engineering Journal*, vol. 436, p. 135190, 2022.

[34] P. Ranieri, G. McGovern, H. Tse, A. Fulmer, M. Kovalenko, G. Nirenberg, V. Miller, A. Rabinovich, A. Fridman, and G. Fridman, “Microsecond-pulsed dielectric barrier discharge plasma-treated mist for inactivation of escherichia coli in vitro,” *IEEE Transactions on Plasma Science*, vol. 47, no. 1, pp. 395–402, 2018.

[35] F. Bilea, C. Bradu, N. Mandache, and M. Magureanu, “Characterization of the chemical activity of a pulsed corona discharge above water,” *Chemosphere*, vol. 236, p. 124302, 2019.

[36] C. Kolb, R. A. Cox, J. Abbatt, M. Ammann, E. Davis, D. Donaldson, B. C. Garrett, C. George, P. Griffiths, D. Hanson, *et al.*, “An overview of current issues in the uptake of atmospheric trace gases by aerosols and clouds,” *Atmospheric Chemistry and Physics*, vol. 10, no. 21, pp. 10561–10605, 2010.

[37] M. Anbar, "The reactions of hydrated electrons with inorganic compounds," *Quarterly Reviews, Chemical Society*, vol. 22, no. 4, pp. 578–598, 1968.

[38] S. A. Norberg, W. Tian, E. Johnsen, and M. J. Kushner, "Atmospheric pressure plasma jets interacting with liquid covered tissue: touching and not-touching the liquid," *Journal of Physics D: Applied Physics*, vol. 47, no. 47, p. 475203, 2014.

[39] S. Mitra, V. Švrček, D. Mariotti, T. Velusamy, K. Matsubara, and M. Kondo, "Microplasma-i nduce liquid chemistry for stabilizing of silicon nanocrystals optical properties in water," *Plasma Processes and Polymers*, vol. 11, no. 2, pp. 158–163, 2014.

[40] L. Chen, C. Iwamoto, E. Omurzak, S. Takebe, H. Okudera, A. Yoshiasa, S. Sulaimankulova, and T. Mashimo, "Synthesis of zirconium carbide (zrc) nanoparticles covered with graphitic "windows" by pulsed plasma in liquid," *RSC advances*, vol. 1, no. 6, pp. 1083–1088, 2011.

[41] S. Sato, K. Mori, O. Ariyada, H. Atsushi, and T. Yonezawa, "Synthesis of nanoparticles of silver and platinum by microwave-induced plasma in liquid," *Surface and Coatings Technology*, vol. 206, no. 5, pp. 955–958, 2011.

[42] J.-K. Lung, J.-C. Huang, D.-C. Tien, C.-Y. Liao, K.-H. Tseng, T.-T. Tsung, W.-S. Kao, T.-H. Tsai, C.-S. Jwo, H.-M. Lin, *et al.*, "Preparation of gold nanoparticles by arc discharge in water," *Journal of alloys and compounds*, vol. 434, pp. 655–658, 2007.

[43] D. Mariotti, J. Patel, V. Švrček, and P. Maguire, "Plasma–liquid interactions at atmospheric pressure for nanomaterials synthesis and surface engineering," *Plasma Processes and Polymers*, vol. 9, no. 11-12, pp. 1074–1085, 2012.

[44] S.-P. Cho, M. A. Bratescu, N. Saito, and O. Takai, “Microstructural characterization of gold nanoparticles synthesized by solution plasma processing,” *Nanotechnology*, vol. 22, no. 45, p. 455701, 2011.

[45] N. Saito, J. Hieda, and O. Takai, “Synthesis process of gold nanoparticles in solution plasma,” *Thin Solid Films*, vol. 518, no. 3, pp. 912–917, 2009.

[46] J. Hieda, N. Saito, and O. Takai, “Exotic shapes of gold nanoparticles synthesized using plasma in aqueous solution,” *Journal of Vacuum Science & Technology A: Vacuum, Surfaces, and Films*, vol. 26, no. 4, pp. 854–856, 2008.

[47] Y.-T. Zhang, Y. Guo, and T.-C. Ma, “Plasma catalytic synthesis of silver nanoparticles,” *Chinese Physics Letters*, vol. 28, no. 10, p. 105201, 2011.

[48] H. Lee, S. H. Park, S.-G. Seo, S.-J. Kim, S.-C. Kim, Y.-K. Park, and S.-C. Jung, “Preparation and characterization of copper nanoparticles via the liquid phase plasma method,” *Current Nanoscience*, vol. 10, no. 1, pp. 7–10, 2014.

[49] H.-G. Kim, H. Lee, B. H. Kim, S.-J. Kim, J.-M. Lee, and S.-C. Jung, “Synthesis process of cobalt nanoparticles in liquid-phase plasma,” *Japanese Journal of Applied Physics*, vol. 52, no. 1S, p. 01AN03, 2013.

[50] N. Amaliyah, S. Mukasa, S. Nomura, H. Toyota, and T. Kitamae, “Plasma in-liquid method for reduction of zinc oxide in zinc nanoparticle synthesis,” *Materials Research Express*, vol. 2, no. 2, p. 025004, 2015.

[51] M. Popp, S. Hann, and G. Koellensperger, “Environmental application of elemental speciation analysis based on liquid or gas chromatography hyphenated to inductively coupled plasma mass spectrometry—a review,” *Analytica Chimica Acta*, vol. 668, no. 2, pp. 114–129, 2010.

[52] F. Rezaei, P. Vanraes, A. Nikiforov, R. Morent, and N. De Geyter, "Applications of plasma-liquid systems: A review," *Materials*, vol. 12, no. 17, p. 2751, 2019.

[53] X. Li, W. Zhou, K. Li, H. Qian, and Z. Ren, "Laser ablation fast pulse discharge plasma spectroscopy analysis of pb, mg and sn in soil," *Optics Communications*, vol. 285, no. 1, pp. 54–58, 2012.

[54] T. Cserfalvi, P. Mezei, and P. Apai, "Emission studies on a glow discharge in atmospheric pressure air using water as a cathode," *Journal of Physics D: Applied Physics*, vol. 26, no. 12, p. 2184, 1993.

[55] M. Magureanu, N. B. Mandache, and V. I. Parvulescu, "Degradation of pharmaceutical compounds in water by non-thermal plasma treatment," *Water research*, vol. 81, pp. 124–136, 2015.

[56] M. Magureanu, C. Bradu, and V. Parvulescu, "Plasma processes for the treatment of water contaminated with harmful organic compounds," *Journal of Physics D: Applied Physics*, vol. 51, no. 31, p. 313002, 2018.

[57] K. H. H. Aziz, H. Miessner, S. Mueller, A. Mahyar, D. Kalass, D. Moeller, I. Khorshid, and M. A. M. Rashid, "Comparative study on 2, 4-dichlorophenoxyacetic acid and 2, 4-dichlorophenol removal from aqueous solutions via ozonation, photocatalysis and non-thermal plasma using a planar falling film reactor," *Journal of hazardous materials*, vol. 343, pp. 107–115, 2018.

[58] N. De Geyter and R. Morent, "Nonthermal plasma sterilization of living and nonliving surfaces," *Annual review of biomedical engineering*, vol. 14, pp. 255–274, 2012.

[59] Y. Yang, Y. I. Cho, and A. Fridman, *Plasma discharge in liquid: water treatment and applications*. CRC press, 2017.

[60] T. Takamatsu, K. Uehara, Y. Sasaki, M. Hidekazu, Y. Matsumura, A. Iwasawa, N. Ito, M. Kohno, T. Azuma, and A. Okino, "Microbial inactivation in the liquid phase induced by multigas plasma jet," *PLoS One*, vol. 10, no. 7, p. e0132381, 2015.

[61] M. J. Pavlovich, H.-W. Chang, Y. Sakiyama, D. S. Clark, and D. B. Graves, "Ozone correlates with antibacterial effects from indirect air dielectric barrier discharge treatment of water," *Journal of Physics D: Applied Physics*, vol. 46, no. 14, p. 145202, 2013.

[62] J. H. Park, N. Kumar, D. H. Park, M. Yusupov, E. Neyts, C. Verlackt, A. Bogaerts, M. H. Kang, H. S. Uhm, E. H. Choi, *et al.*, "A comparative study for the inactivation of multidrug resistance bacteria using dielectric barrier discharge and nano-second pulsed plasma. sci. rep. 5 (2015)."

[63] Y. Gorbanev, D. O'Connell, and V. Chechik, "Non-thermal plasma in contact with water: The origin of species," *Chemistry–A European Journal*, vol. 22, no. 10, pp. 3496–3505, 2016.

[64] G. Fridman, G. Friedman, A. Gutsol, A. B. Shekhter, V. N. Vasilets, and A. Fridman, "Applied plasma medicine," *Plasma processes and polymers*, vol. 5, no. 6, pp. 503–533, 2008.

[65] B. Surowsky, O. Schlüter, and D. Knorr, "Interactions of non-thermal atmospheric pressure plasma with solid and liquid food systems: a review," *Food Engineering Reviews*, vol. 7, no. 2, pp. 82–108, 2015.

[66] T. Ohta, "Plasma in agriculture. cold plasma in food and agriculture," 2016.

[67] L. Sivachandiran and A. Khacef, "Enhanced seed germination and plant growth by atmospheric pressure cold air plasma: combined effect of seed and water treatment," *RSC advances*, vol. 7, no. 4, pp. 1822–1832, 2017.

[68] P. G. Subramanian, H. Rao, A. M. Shivapuji, P.-L. Girard-Lauriault, and L. Rao, “Plasma-activated water from dbd as a source of nitrogen for agriculture: Specific energy and stability studies,” *Journal of Applied Physics*, vol. 129, no. 9, p. 093303, 2021.

[69] B. Jiang, J. Zheng, and M. Wu, “Nonthermal plasma for effluent and waste treatment,” in *Cold Plasma in Food and Agriculture*, pp. 309–342, Elsevier, 2016.

[70] R. Zhou, R. Zhou, X. Zhang, J. Zhuang, S. Yang, K. Bazaka, *et al.*, “Effects of atmospheric-pressure n2, he, air, and o2 microplasmas on mung bean seed germination and seedling growth,” *Scientific reports*, vol. 6, no. 1, pp. 1–11, 2016.

[71] J. D. Holladay, J. Hu, D. L. King, and Y. Wang, “An overview of hydrogen production technologies,” *Catalysis today*, vol. 139, no. 4, pp. 244–260, 2009.

[72] D. H. Lee, K.-T. Kim, Y.-H. Song, W. S. Kang, and S. Jo, “Mapping plasma chemistry in hydrocarbon fuel processing processes,” *Plasma Chemistry and Plasma Processing*, vol. 33, no. 1, pp. 249–269, 2013.

[73] W. Sun, M. Uddi, S. H. Won, T. Ombrello, C. Carter, and Y. Ju, “Kinetic effects of non-equilibrium plasma-assisted methane oxidation on diffusion flame extinction limits,” *Combustion and Flame*, vol. 159, no. 1, pp. 221–229, 2012.

[74] E. Mintoussov, S. Pancheshnyi, and A. Starikovskii, “Propane-air flame control by non-equilibrium low-temperature pulsed nanosecond barrier discharge,” in *42nd AIAA Aerospace Sciences Meeting and Exhibit*, p. 1013, 2004.

[75] Y. Kim, W. S. Kang, J. M. Park, S. H. Hong, Y.-H. Song, and S. J. Kim, “Experimental and numerical analysis of streamers in pulsed corona and dielectric barrier discharges,” *IEEE transactions on plasma science*, vol. 32, no. 1, pp. 18–24, 2004.

[76] S. Kado, K. Urasaki, Y. Sekine, K. Fujimoto, T. Nozaki, and K. Okazaki, "Reaction mechanism of methane activation using non-equilibrium pulsed discharge at room temperature," *Fuel*, vol. 82, no. 18, pp. 2291–2297, 2003.

[77] S. Yao, F. Ouyang, A. Nakayama, E. Suzuki, M. Okumoto, and A. Mizuno, "Oxidative coupling and reforming of methane with carbon dioxide using a high-frequency pulsed plasma," *Energy & Fuels*, vol. 14, no. 4, pp. 910–914, 2000.

[78] C. De Bie, B. Verheyde, T. Martens, J. van Dijk, S. Paulussen, and A. Bogaerts, "Fluid modeling of the conversion of methane into higher hydrocarbons in an atmospheric pressure dielectric barrier discharge," *Plasma Processes and Polymers*, vol. 8, no. 11, pp. 1033–1058, 2011.

[79] K. K. Kuo, "Principles of combustion," 1986.

[80] D. H. Lee, K.-T. Kim, M. S. Cha, and Y.-H. Song, "Plasma-controlled chemistry in plasma reforming of methane," *International Journal of Hydrogen Energy*, vol. 35, no. 20, pp. 10967–10976, 2010.

[81] C.-j. Liu, R. Mallinson, and L. Lobban, "Nonoxidative methane conversion to acetylene over zeolite in a low temperature plasma," *Journal of catalysis*, vol. 179, no. 1, pp. 326–334, 1998.

[82] M. Heintze, M. Magureanu, and M. Kettlitz, "Mechanism of c 2 hydrocarbon formation from methane in a pulsed microwave plasma," *Journal of applied physics*, vol. 92, no. 12, pp. 7022–7031, 2002.

[83] T. Nozaki, A. Hattori, and K. Okazaki, "Partial oxidation of methane using a microscale non-equilibrium plasma reactor," *Catalysis today*, vol. 98, no. 4, pp. 607–616, 2004.

[84] V. Goujard, T. Nozaki, S. Yuzawa, A. Ağiral, and K. Okazaki, "Plasma-assisted partial oxidation of methane at low temperatures: numerical analysis of gas-phase chemical mechanism," *Journal of Physics D: Applied Physics*, vol. 44, no. 27, p. 274011, 2011.

[85] G. SriBala, D. Michiels, C. Leys, K. M. Van Geem, G. B. Marin, and A. Nikiforov, "Methane reforming to valuable products by an atmospheric pressure direct current discharge," *Journal of cleaner production*, vol. 209, pp. 655–664, 2019.

[86] N. Khadir, K. Khodja, and A. Belasri, "Methane conversion using a dielectric barrier discharge reactor at atmospheric pressure for hydrogen production," *Plasma Science and Technology*, vol. 19, no. 9, p. 095502, 2017.

[87] H. Zhang, F. Zhu, Z. Bo, K. Cen, and X. Li, "Hydrogen production from methanol decomposition in a gliding arc discharge plasma with high processing capacity," *Chemistry Letters*, vol. 44, no. 10, pp. 1315–1317, 2015.

[88] R. Shiraishi, S. Nomura, S. Mukasa, R. Nakano, and R. Kamatoko, "Effect of catalytic electrode and plate for methanol decomposition by in-liquid plasma," *International Journal of Hydrogen Energy*, vol. 43, no. 9, pp. 4305–4310, 2018.

[89] T. Zhu, B. Sun, X. Zhu, L. Wang, Y. Xin, and J. Liu, "Mechanism analysis of hydrogen production by microwave discharge in ethanol liquid," *Journal of Analytical and Applied Pyrolysis*, vol. 156, p. 105111, 2021.

[90] X. Zhu, T. Hoang, L. L. Lobban, and R. G. Mallinson, "Plasma steam reforming of e85 for hydrogen rich gas production," *Journal of Physics D: Applied Physics*, vol. 44, no. 27, p. 274002, 2011.

[91] B. Ulejczyk, Ł. Nogal, M. Młotek, and K. Krawczyk, "Hydrogen production from ethanol using dielectric barrier discharge," *Energy*, vol. 174, pp. 261–268, 2019.

[92] Y. Ma, J. D. Harding, and X. Tu, "Catalyst-free low temperature conversion of n-dodecane for co-generation of cox-free hydrogen and c2 hydrocarbons using a gliding arc plasma," *International Journal of Hydrogen Energy*, vol. 44, no. 48, pp. 26158–26168, 2019.

[93] Z. Wu, W. Zhou, X. Hao, and X. Zhang, "Plasma reforming of n-pentane as a simulated gasoline to hydrogen and cleaner carbon-based fuels," *Energy*, vol. 189, p. 116265, 2019.

[94] J. Gonzalez-Aguilar, G. Petitpas, A. Lebouvier, J.-D. Rollier, A. Darmon, and L. Fulcheri, "Three stages modeling of n-octane reforming assisted by a nonthermal arc discharge," *Energy & fuels*, vol. 23, no. 10, pp. 4931–4936, 2009.

[95] X. Zhang and M. S. Cha, "Tailored reforming of n-dodecane in an aqueous discharge reactor," *Journal of Physics D: Applied Physics*, vol. 49, no. 17, p. 175201, 2016.

[96] S. M. Thagard, G. Prieto, K. Takashima, and A. Mizuno, "Identification of gas-phase by-products formed during electrical discharges in liquid fuels," *IEEE Transactions on Plasma Science*, vol. 40, no. 9, pp. 2106–2111, 2012.

[97] Y. Matsui, S. Kawakami, K. Takashima, S. Katsura, and A. Mizuno, "Liquid-phase fuel re-forming at room temperature using nonthermal plasma," *Energy & fuels*, vol. 19, no. 4, pp. 1561–1565, 2005.

[98] M. A. Malik, D. Hughes, A. Malik, S. Xiao, and K. H. Schoenbach, "Study of the production of hydrogen and light hydrocarbons by spark discharges in diesel, kerosene, gasoline, and methane," *Plasma Chemistry and Plasma Processing*, vol. 33, no. 1, pp. 271–279, 2013.

[99] M. R. Khani, S. H. R. Barzoki, M. S. Yaghmaee, S. I. Hosseini, M. Shariat, B. Shokri, A. R. Fakhari, S. Nojavan, H. Tabani, and M. Ghaedian, "Investigation of cracking by cylindrical dielectric barrier discharge reactor on the n-hexadecane as a model

compound," *IEEE Transactions on Plasma Science*, vol. 39, no. 9, pp. 1807–1813, 2011.

[100] H. Taghvaei, A. Jahanmiri, M. R. Rahimpour, M. M. Shirazi, and N. Hooshmand, "Hydrogen production through plasma cracking of hydrocarbons: Effect of carrier gas and hydrocarbon type," *Chemical Engineering Journal*, vol. 226, pp. 384–392, 2013.

[101] T. Paulmier and L. Fulcheri, "Use of non-thermal plasma for hydrocarbon reforming," *Chemical engineering journal*, vol. 106, no. 1, pp. 59–71, 2005.

[102] S. Sadrameli, "Thermal/catalytic cracking of liquid hydrocarbons for the production of olefins: A state-of-the-art review ii: Catalytic cracking review," *Fuel*, vol. 173, pp. 285–297, 2016.

[103] Z. Xiao, C. Wu, L. Li, G. Li, G. Liu, and L. Wang, "Pursuing complete and stable steam reforming of n-dodecane over nickel catalysts at low temperature and high lhsv," *International Journal of Hydrogen Energy*, vol. 42, no. 8, pp. 5606–5618, 2017.

[104] L. G. A. Borges, A. Savi, C. Teixeira, R. P. de Oliveira, M. L. F. De Camillis, R. Wickert, S. F. M. Brodt, T. F. Tonietto, R. Cremonese, L. S. da Silva, *et al.*, "Mechanical ventilation weaning protocol improves medical adherence and results," *Journal of critical care*, vol. 41, pp. 296–302, 2017.

[105] A. Starikovskiy, Y. Yang, Y. I. Cho, and A. Fridman, "Non-equilibrium plasma in liquid water: dynamics of generation and quenching," *Plasma Sources Science and Technology*, vol. 20, no. 2, p. 024003, 2011.

[106] J. C. Whitehead and M. Prantsidou, "Investigation of hydrocarbon oil transformation by gliding arc discharge: comparison of batch and recirculated configurations," *Journal of Physics D: Applied Physics*, vol. 49, no. 15, p. 154001, 2016.

[107] Y. A. Lebedev, A. Tatarinov, and I. Epstein, “On the role of electron impact in an atmospheric-pressure microwave discharge in liquid n-heptane,” *Plasma Physics Reports*, vol. 43, no. 4, pp. 510–513, 2017.

[108] J.-P. Liang, Z.-L. Zhao, X.-F. Zhou, D.-Z. Yang, H. Yuan, W.-C. Wang, and J.-J. Qiao, “Comparison of gas phase discharge and gas-liquid discharge for water activation and methylene blue degradation,” *Vacuum*, vol. 181, p. 109644, 2020.

[109] P. Vanraes and A. Bogaerts, “The essential role of the plasma sheath in plasma–liquid interaction and its applications—a perspective,” *Journal of Applied Physics*, vol. 129, no. 22, p. 220901, 2021.

[110] S. Bresch, R. Wandell, H. Wang, I. Alabugin, and B. R. Locke, “Oxidized derivatives of n-hexane from a water/argon continuous flow electrical discharge plasma reactor,” *Plasma Chemistry and Plasma Processing*, vol. 36, no. 2, pp. 553–584, 2016.

[111] H. Zhang, X. Li, F. Zhu, K. Cen, C. Du, and X. Tu, “Plasma assisted dry reforming of methanol for clean syngas production and high-efficiency co2 conversion,” *Chemical engineering journal*, vol. 310, pp. 114–119, 2017.

[112] I. Kosarev, N. Aleksandrov, S. Kindysheva, S. Starikovskaia, and A. Y. Starikovskii, “Kinetics of ignition of saturated hydrocarbons by nonequilibrium plasma: Ch4-containing mixtures,” *Combustion and flame*, vol. 154, no. 3, pp. 569–586, 2008.

[113] R. G. Pierce, G. Padron-Wells, and M. J. Goeckner, “Gas-phase chemistry of pulsed n-hexane discharge,” *Plasma Chemistry and Plasma Processing*, vol. 29, no. 1, pp. 1–11, 2009.

[114] C. F. Association *et al.*, “The economics of petroleum refining,” *Understanding the business of processing crude oil into fuels and other value added products.[Online] Available at: http://www. canadianfuels.*

ca/website/media/PDF/Publications/Economics-fundamentals0of-Refiningd-December-2013-Final-English. pdf, 2013.

[115] J. Weitkamp, "Catalytic hydrocracking—mechanisms and versatility of the process," *ChemCatChem*, vol. 4, no. 3, pp. 292–306, 2012.

[116] M. E. C. Puertas, *Nanosecond-pulsed pin-to-liquid discharges for the degradation of recalcitrant aqueous organic pollutants.* McGill University (Canada), 2021.

[117] D. Rusterholtz, *Nanosecond repetitively pulsed discharges in atmospheric pressure air.* PhD thesis, Ecole Centrale Paris, 2012.

[118] H. Sun, S. Zhang, Y. Gao, C. Zhang, and T. Shao, "Self-heating effect on stability of a nanosecond pulsed dbd interacting with heptane and methylnaphthalene as heavy oil model compounds," *IEEE Transactions on Dielectrics and Electrical Insulation*, vol. 26, no. 2, pp. 431–438, 2019.

[119] F. I. Mopsik, "Dielectric constant of n-hexane as a function of temperature, pressure, and density," *Journal of Research of the National Bureau of Standards. Section A, Physics and Chemistry*, vol. 71, no. 4, p. 287, 1967.

[120] M. Mohsen-Nia, H. Amiri, and B. Jazi, "Dielectric constants of water, methanol, ethanol, butanol and acetone: measurement and computational study," *Journal of Solution Chemistry*, vol. 39, no. 5, pp. 701–708, 2010.

[121] J. C. Brown and E. Gulari, "Hydrogen production from methanol decomposition over pt/al2o3 and ceria promoted pt/al2o3 catalysts," *Catalysis Communications*, vol. 5, no. 8, pp. 431–436, 2004.

[122] M. Jimenez, R. Rincon, A. Marinas, and M. Calzada, "Hydrogen production from ethanol decomposition by a microwave plasma: Influence of the plasma gas flow," *International journal of hydrogen energy*, vol. 38, no. 21, pp. 8708–8719, 2013.

[123] Y. Cao, Z. Gao, J. Jin, H. Zhou, M. Cohron, H. Zhao, H. Liu, and W. Pan, “Synthesis gas production with an adjustable h2/co ratio through the coal gasification process: effects of coal ranks and methane addition,” *Energy & fuels*, vol. 22, no. 3, pp. 1720–1730, 2008.

[124] B. B. Sahoo, N. Sahoo, and U. K. Saha, “Effect of h2: Co ratio in syngas on the performance of a dual fuel diesel engine operation,” *Applied Thermal Engineering*, vol. 49, pp. 139–146, 2012.